RM E 56 F 28b

NACA RM E56F28b

Copy
RM E56F28b

CLASSIFIED

NACA

RESEARCH MEMORANDUM

ALTITUDE FREE-JET INVESTIGATION OF DYNAMICS OF A 28-INCH-DIAMETER RAM-JET ENGINE

By Carl B. Wentworth, William R. Dunbar, and Robert J. Crowl

Lewis Flight Propulsion Laboratory
Cleveland, Ohio

DECLASSIFIED
NASA CLASS. CHANGE NOTICE
Issue No. 2/2
Date 1-29-71
fer ma

LIBRARY
JAN 16 1957
LEWIS LIBRARY, NACA
CLEVELAND, OHIO

CLASSIFIED DOCUMENT

This material contains information affecting the National Defense of the United States within the meaning of the espionage laws, Title 18, U.S.C., Secs. 793 and 794, the transmission or revelation of which in any manner to an unauthorized person is prohibited by law.

NATIONAL ADVISORY COMMITTEE
FOR AERONAUTICS

WASHINGTON

January 15, 1957

NACA RM E56F28b

[redacted]

NATIONAL ADVISORY COMMITTEE FOR AERONAUTICS

RESEARCH MEMORANDUM

ALTITUDE FREE-JET INVESTIGATION OF DYNAMICS OF A 28-INCH-DIAMETER RAM-JET ENGINE

By Carl B. Wentworth, William R. Dunbar, and Robert J. Crowl

4058

T-13

SUMMARY

The dynamic response of a 28-inch-diameter ram-jet engine was determined for flight Mach numbers of 2.35 and 2.50 and altitudes of 50,000, 60,000, and 65,000 feet. It was found that the response of engine pressures to fuel flow disturbances can be described by the linear transfer function

$$G = e^{-t_d s}\left(\frac{1 + \sigma\tau_1 s}{1 + \tau_1 s}\right)\left(\frac{1}{1 + \tau_2 s}\right)$$

where t_d is dead time, s is the Laplace operator, σ is the rise ratio, and τ_1 and τ_2 are time constants.

Values of t_d ranged from 0.005 to 0.035 second, and σ had values from 0.67 (-3.5 db) to 1.0 (0 db). The lag factor $\frac{1}{1 + \tau_2 s}$ was encountered only when the range of fuel flow oscillations extended into the subcritical regime of diffuser operation.

INTRODUCTION

The feasibility of closed-loop control of ram-jet-engine thrust is demonstrated in references 1 and 2. In each case the control system relies upon the relation between engine thrust and a pressure measured in the subsonic portion of the inlet diffuser.

The design of the closed-loop control equipment is greatly expedited if the dynamic characteristics of the engine to be controlled are adequately known. Present literature does not provide sufficient

[redacted]

information to allow estimation of the dynamic response of all ram-jet engines. Accordingly, each engine for which a control is desired must be evaluated dynamically by experimental means.

The dynamic behavior of a 28-inch-diameter ram-jet engine designed to operate in the Mach number range of 2.35 to 2.70 is evaluated herein. The investigation was conducted with a heavy-duty water-jacketed engine operated in an altitude free-jet facility. Simulated altitudes of 50,000, 60,000, and 65,000 feet at jet Mach numbers of 2.35 and 2.50 were used. The dynamic response was obtained at angles of attack of zero and $\pm 7^{\circ}$.

4058

The frequency response of engine pressures to sinusoidal variations of fuel flow was found for frequencies from 0.1 to 50 cps. The dead time of engine pressures to fuel flow was found by making step disturbances in fuel flow.

SYMBOLS

The following symbols are used in this report:

A_f	ratio of fuel flow amplitude to its amplitude at low frequency ($f < 0.1$)
A_p	ratio of pressure amplitude to its amplitude at low frequency ($f < 0.1$)
f	frequency, cps
f/a	engine fuel-air ratio
G	linear transfer function relating pressure response to fuel flow disturbances
P	total pressure at engine diffuser outlet, lb/sq ft
p_0	static pressure in jet (simulated altitude static pressure), lb/sq ft
s	Laplace operator
t_d	dead time (time lapse between fuel disturbance and its effect on engine pressure), sec
σ	rise ratio of transfer function G

τ_1 time constant of lead-lag part of transfer function G, sec

τ_2 time constant of lag part of transfer function G, sec

APPARATUS AND PROCEDURE

Facility

The altitude free-jet facility with the engine installed is shown in figure 1. The engine inlet is submerged in an air jet issuing from the supersonic nozzle. Two interchangeable nozzles provided test Mach numbers of 2.35 and 2.50 and could be rotated about a horizontal pivot perpendicular to the plane of the sketch to provide simulation of angles of attack from $+7^{\circ}$ to -7°. Inlet air was heated to appropriate temperatures by gas-fired heat exchangers. The pressure in the compartment containing the engine was always low enough to ensure choked flow in the engine exhaust nozzle.

Engine

The engine tested is shown in greater detail in figure 2. The combustion-chamber diameter at its largest section was 28 inches. The supersonic portion of the inlet had a single cone and was designed to have the conical shock wave at the cowl lip at a Mach number of 2.50. The minimum exhaust-nozzle area was 0.70 times the maximum combustion-chamber area. The internal-flow areas are presented in figure 3, where area is plotted against station.

The engine was equipped with two independent sets of variable-area spring-loaded fuel nozzles. One set, called the inner ring, was supplied with fuel equivalent to an over-all fuel-air ratio of 0.037, and this ratio was constant for all the runs presented herein. The other set, called the outer ring, was used to provide the prescribed fuel variations.

External Fuel System

The modulation of the outer-ring fuel flow was accomplished by means of an electrohydraulic valve designed according to the principles presented in references 3 and 4. The valve and associated piping were capable of producing step disturbances in engine fuel flow which were completed in 0.02 second. Step disturbances were made by a switch that varied the voltage supplied to the valve. Sinusoidal variations were achieved by means of a sine-wave signal generator.

Instrumentation

Steady state. - The location of the steady-state pressure instrumentation is also shown in figure 2. Pressures were measured with mercury manometers and the measurements were used to define the base values of engine diffuser pressure recovery and to calibrate the transient instrumentation. The temperature of the inlet air was measured with thermocouples. Steady-state fuel flow was measured with a turbine-type electronic flowmeter.

Transient. - Fast-response transducers were used to measure pressures during transients. The electric output of the transducers was applied to a recording galvanometer. The transducers and galvanometers had flat response (±5 percent) for frequencies up to 40 cps. Phase shift was less than 30° at 40 cps. The transducers were used to measure wall static pressures at the locations shown in figure 2.

Transient fuel flow was established by the fuel-manifold pressure. The relation between fuel flow and manifold pressure was essentially linear because of the design of the spring-loaded variable-area fuel nozzles. Fuel flow response to manifold pressure was found to be flat within ±5 percent to approximately 40 cps, and the phase shift was approximately 30° at 40 cps.

Procedure

The investigation was conducted at simulated flight Mach numbers of 2.35 and 2.50 and altitudes of 50,000, 60,000, and 65,000 feet. The free-jet total temperature was maintained at 358° F for the tests at a Mach number of 2.35 and at 415° F for the tests at a Mach number of 2.50.

Data were obtained by imposing step or sinusoidal disturbances of various sizes upon base fuel flows of various magnitudes. The sinusoidal fuel inputs were used to determine the frequency response of diffuser static pressures to fuel flow. Step inputs were utilized to determine the dead time of engine pressures to fuel flow and to study the influence of various parameters upon dead time.

It is estimated that values of amplitude ratio and phase lag from the frequency-response data are within ±1 decibel and $\pm 15^{\circ}$ of the correct values, respectively. Values of dead time are estimated to be within ±0.002 second of the correct value.

RESULTS AND DISCUSSION

Dynamic Response to Sinusoidal Fuel Variations

Base points and amplitudes. - The variation of diffuser pressures with fuel flow is presented in figure 4. The solid lines were obtained with an X-Y recorder as the fuel flow was increased and decreased with a triangular input at 0.01 cps. This frequency is low enough that the lines can be considered as a steady-state calibration. The symbols represent steady-state manometer readings. The dashed curves were faired through the symbols in those cases where data were not obtained with the X-Y recorder.

4058

Three sinusoidal input tests were run at an altitude of 60,000 feet for Mach numbers of 2.35 and 2.50. The horizontal bars on figure 4 represent the amplitude of the sinusoidal fuel variation about the base point indicated by the vertical line for each of the tests. For each Mach number, two sets of frequency-response data of the same amplitude were obtained at different diffuser pressure-recovery ratios P_2/p_0. Another set of frequency-response data of larger amplitude was obtained at the same diffuser pressure-recovery ratio as the lower of the small-amplitude tests.

The steady-state pressure curves in figure 4 are decidedly nonlinear. Because of this nonlinearity, the pressure response to sinusoidal fuel input will not itself be sinusoidal. To illustrate this, the distortion of wave form is shown in figure 5 for a fuel variation corresponding to the 0.038 fuel-air ratio amplitude sinusoid at a Mach number of 2.50. Although linear transfer functions are applied to the frequency-response data, it should be noted that such application is not completely proper. The error involved is less for the smaller-amplitude sinusoids.

A typical example of frequency-response data obtained for engine operation at a Mach number of 2.50 and an altitude of 60,000 feet is presented in figure 6.

Effect of base recovery. - The frequency response for a small-amplitude fuel input at a low base diffuser pressure recovery is presented in figure 7 for Mach numbers of 2.35 and 2.50. The amplitude ratio and the phase lag are plotted against frequency for two diffuser stations. The amplitude ratio is given in decibels where

$$\text{Amplitude ratio (db)} = 20 \log_{10} \frac{A_p}{A_f}$$

Curves of the linear transfer functions and their straight-line approximations have been fitted to the data. Time constants were obtained from the corner frequencies of the straight-line approximation, where $\tau_{1,2} = \frac{1}{2\pi f}$.

The data of figure 7 are adequately represented by a lead-lag transfer function with dead time:

$$G = e^{-t_d s}\left(\frac{1 + \sigma\tau_1 s}{1 + \tau_1 s}\right)$$

where σ is approximately -3 db (0.7), and τ_1 has values from 0.021 to 0.23 second.

The frequency response for an input of the same amplitude but at a high base recovery is presented in figure 8 for three diffuser stations. At a flight Mach number of 2.50 (figs. 8(a), (b), and (c)), the data show an additional lag factor giving a transfer function

$$G = e^{-t_d s}\left(\frac{1 + \sigma\tau_1 s}{1 + \tau_1 s}\right)\left(\frac{1}{1 + \tau_2 s}\right)$$

The data for a Mach number of 2.35 (figs. 8(d), (e), and (f)) can be considered as a lead-lag transfer function with dead time if the response at station 24 is interpreted to have a rise ratio σ of 0 decibel (1.0). The data do not extend beyond 10 cps, so the existence of a lag factor is not determined. Values of σ range from -2.5 to 0 decibel (0.75 to 1.0); τ_1 has values from 0.028 to 0.25 second; and the time constant τ_2 ranges from 0.0043 to 0.009 second.

Figures 7 and 8, therefore, show that a lead-lag response occurs at both high and low base pressure recoveries, but an additional lag factor is present at the high base pressure recovery.

Effect of amplitude. - The frequency response to a large-amplitude input with a low base pressure recovery is presented in figure 9. For a Mach number of 2.50 (figs. 9(a), (b), and (c)), the response can be represented as a lag with dead time. However, as with figures 8(d), (e), and (f), the transfer function can be given as

$$G = e^{-t_d s}\left(\frac{1 + \sigma\tau_1 s}{1 + \tau_1 s}\right)\left(\frac{1}{1 + \tau_2 s}\right)$$

where σ is 1.0 (0 db).

At a Mach number of 2.35 (figs. 9(d), (e), and (f)), the data do not extend to frequencies above 10 cps, and, again, it is not possible to confirm the existence of a lag factor.

Values of σ range from -3.5 (0.67) to 0 decibel (1.0) for the large-amplitude low-base-pressure-recovery input. The time constant τ_1 has values from 0.057 to 0.18 second; τ_2 ranges from 0.0165 to 0.02 second.

A comparison of small and large amplitudes at the low base pressure recovery (figs. 7 and 9, respectively) reveals that the larger amplitude has a lag response not present at the smaller amplitude. The same lag response also occurs for the small amplitude at high base pressure recovery (fig. 8). Therefore, the occurrence of the lag factor is not related to base pressure recovery alone nor to amplitude alone. The data of figures 8 and 9, however, have one thing in common which is revealed in figure 4. Both sinusoids extend well into the subcritical regime of diffuser pressure-recovery ratios. Thus, the occurrence of the lag response appears to be related to subcritical operation.

Effect of altitude. - Sets of frequency-response data corresponding to the high-base-pressure-recovery small-amplitude sinusoid were obtained at altitudes of 50,000 and 65,000 feet for a Mach number of 2.50 and are presented in figure 10 with the data for an altitude of 60,000 feet (figs. 8(a), (b), and (c)). The data for altitudes of 50,000 and 65,000 feet are adequately represented by a lag term, whereas the data for 60,000 feet have a lead-lag term with a rise ratio of -2.5 decibels as well. Despite these differences, the curve shapes are about the same. However, the time constant τ_2 does not vary consistently with altitude so that the effect of altitude, if any exists, is obscure. Values of τ_2 range from 0.004 to 0.0398 second. The fuel flow oscillations at each altitude extend into the subcritical regime, thus corroborating the relation between the occurrence of the lag response and subcritical operation referred to in the discussion of figures 8 and 9 in the preceding section.

Frequency response at angle of attack. - Sets of frequency-response data were obtained at angles of attack of $\pm 7^{\circ}$. Because no appreciable difference existed between the data at these two angles of attack, only the set for $+7^{\circ}$ are presented in figure 11, which shows the steady-state values of pressure for various fuel flows and the base point and amplitude of fuel flow.

The frequency-response data for a sinusoidal fuel input for an angle of attack of $+7^{\circ}$ are presented in figure 12. The response is characterized by a lag behavior at all three pressure locations. It is noted in figure 11 that the diffuser was operated into the subcritical

regime, thus presenting further evidence of a connection between subcritical operation and the occurrence of the lag response. The time constants of the lag terms range from 0.006 second at station 24 to 0.0173 second at station 68.

Dead Time Determined from Fuel Flow Step Disturbances

Although values of dead time were obtained from the frequency-response data, the number of base points, amplitudes, and pressure locations for which data were obtained was severely limited by the nature of the tests. Further measurements of dead time were obtained by subjecting the engine to step disturbances in fuel flow. Dead time was then measured as the time interval between the step in fuel flow and the corresponding change in pressure at the engine station for which the dead time was desired. Dead-time data could be obtained more rapidly by this method than by the frequency-response method. Consequently, the step-input method was used to explore the effects of various parameters upon dead time.

4058

Dead-time variation through the engine. - Dead times at various stations in the engine are presented in figure 13 for step increases and decreases from the same base point. It is evident that dead time tends to be minimum at axial locations between the flameholder (station 78) and the exhaust-nozzle minimum area (station 144). The heavy solid line on figure 13(a) indicates the approximate time required for movement of the fuel step from the injector (station 50) to the combustion zone. The intersection of the dashed line with the dead-time curve should represent the station of minimum dead time. The fuel transport velocity for stations downstream of the flameholder is not known because of the difficulty in measuring the velocity in the burning zone. For this reason, the intersection of the two curves can only be estimated. It is clear, however, that the point of minimum dead time is quite different for step increases than for step decreases because of the separation between the two dead-time curves (fig. 13(a)).

A method of estimating the dead time of ram-jet engines is published in reference 5. The dead time is computed as a fuel travel time (at the gas velocity) and an upstream wave propagation time. The station where the fuel step is transformed (by burning) to a pressure step is assumed to be at the exhaust-nozzle minimum area. This method gives dead times greater than were measured herein and does not account for the variations in the station at which the pressure wave originates. However, the propagation rates assumed in reference 5 (gas velocity for downstream movement of fuel and acoustic velocity minus gas velocity for pressure-wave movement upstream) are in essential agreement with the data presented herein.

The dead time for step decreases is greater than for step increases at Mach numbers of 2.50 and 2.35 (fig. 13). The curves for step increases and decreases appear to be nearly parallel, suggesting that the rates of forward movement of the pressure step are equal. The difference in level of the two curves must then be due to differences in the station where the pressure wave originates, which, in turn, must be a matter of combustion dynamics.

It should be pointed out that the dead time at stations near the cowl (station 0) will be infinite, if the shock wave is downstream of the pressure-measuring hole throughout the transient. The step-decrease transient of figure 13(a) is an example of this for the pressure at stations 0 and 1.

Effect of diffuser pressure-recovery ratio upon dead time. - The effect of diffuser pressure-recovery ratio upon dead time is presented in figure 14. The dead time for a Mach number of 2.50 (fig. 14(a)) shows a decreasing trend as the diffuser pressure-recovery ratio is increased. Flow velocities in the diffuser decrease as the pressure-recovery ratio is increased. This decrease of flow velocity affords greater forward pressure-wave propagation speeds, which would give the observed trend of decreasing dead time with increasing diffuser pressure recovery. At the same time, the possibility exists that the rate of combustion of the new fuel increment may vary with base fuel-air ratio, which is different at each pressure recovery. Of these two possible explanations, the first should be manifested by changes in the slope of the curves of dead time against axial station. Differences in combustion rate would be evidenced by shifting of the curves in the direction of increasing or decreasing dead time. It appears in figure 14(a) that the propagation rate changes markedly at low diffuser pressure recoveries, but in the higher range of pressure recoveries the combustion-rate effect predominates.

At a Mach number of 2.35 (fig. 14(b)), the effect of base diffuser pressure recovery is almost negligible.

Effect of step size on dead time. - The effect of step size upon dead time is presented in figure 15. For step increases at a low base recovery (fig. 15(a)), variations in dead time are small. At higher base recovery (fig. 15(b)), step decreases show a significant range of dead times with step size. The curves are essentially parallel; so it can be inferred that the difference is due to combustion phenomena rather than the propagation rate. In figure 15(c), the effect of step size is shown for a relatively high pressure recovery and step increases. Doubling the step size increases the dead time about 50 percent. Again, the effect appears to be related to combustion rather than propagation rate.

CONCLUDING REMARKS

The dynamic response to fuel-flow disturbances of a 28-inch-diameter ram-jet engine was found to be represented by a transfer function of the type

$$G = e^{-t_d s}\left(\frac{1 + \sigma\tau_1 s}{1 + \tau_1 s}\right)\left(\frac{1}{1 + \tau_2 s}\right)$$

where t_d is dead time, s is the Laplace operator, σ is the rise ratio, and τ_1 and τ_2 are time constants. Values of t_d ranged from 0.005 to 0.035 second. The following trends in dead time were observed:

1. Dead time was found to have a minimum value at an engine station between the flameholder and the exhaust-nozzle minimum area station, and it increased in both upstream and downstream directions.

2. Step increases in fuel flow had dead times slightly shorter than did step decreases.

3. Dead time was found to decrease as diffuser-exit total-pressure recovery ratio increased.

4. Dead time increased as the size of the fuel-flow disturbances increased. This trend appeared to be the result of combustion dynamics.

Values of σ ranged from 0.67 (-3.5 db) to 1.0 (0 db). No trend in rise ratio with other variables could be determined from the data.

Values of τ_1 varied from 0.02 to 0.25 second.

The lag factor $\frac{1}{1 + \tau_2 s}$ in the transfer function occurred only when the range of fuel flow oscillations extended into the subcritical regime of diffuser operation. Values of τ_2 ranged from 0.005 to 0.02 second.

National Advisory Committee for Aeronautics
Lewis Flight Propulsion Laboratory
Cleveland, Ohio, July 17, 1956

REFERENCES

1. Dunbar, William R., Vasu, George, and Hurrell, Herbert G.: Experimental Investigation of Direct Control of Diffuser Pressure on 16-Inch Ram-Jet Engine. NACA RM E55D15, 1955.

2. Vasu, George, Hart, Clint E., and Dunbar, William R.: Preliminary Report on Experimental Investigation of Engine Dynamics and Controls for a 48-Inch Ram-Jet Engine. NACA RM E55J12, 1956.

3. Gold, Harold, Otto, Edward W., and Ransom, Victor L.: Dynamics of Mechanical Feedback-Type Hydraulic Servomotors under Inertia Loads. NACA Rep. 1125, 1953. (Supersedes NACA TN 2767.)

4. Otto, Edward W., Gold, Harold, and Hiller, Kirby W.: Design and Performance of Throttle-Type Fuel Controls for Engine Dynamic Studies. NACA TN 3445, 1955.

5. Wilcox, Fred A., and Anderson, Arthur R.: An Analysis of Ram-Jet Engine Time Delay Following a Fuel-Flow Disturbance. NACA RM E55D22, 1955.

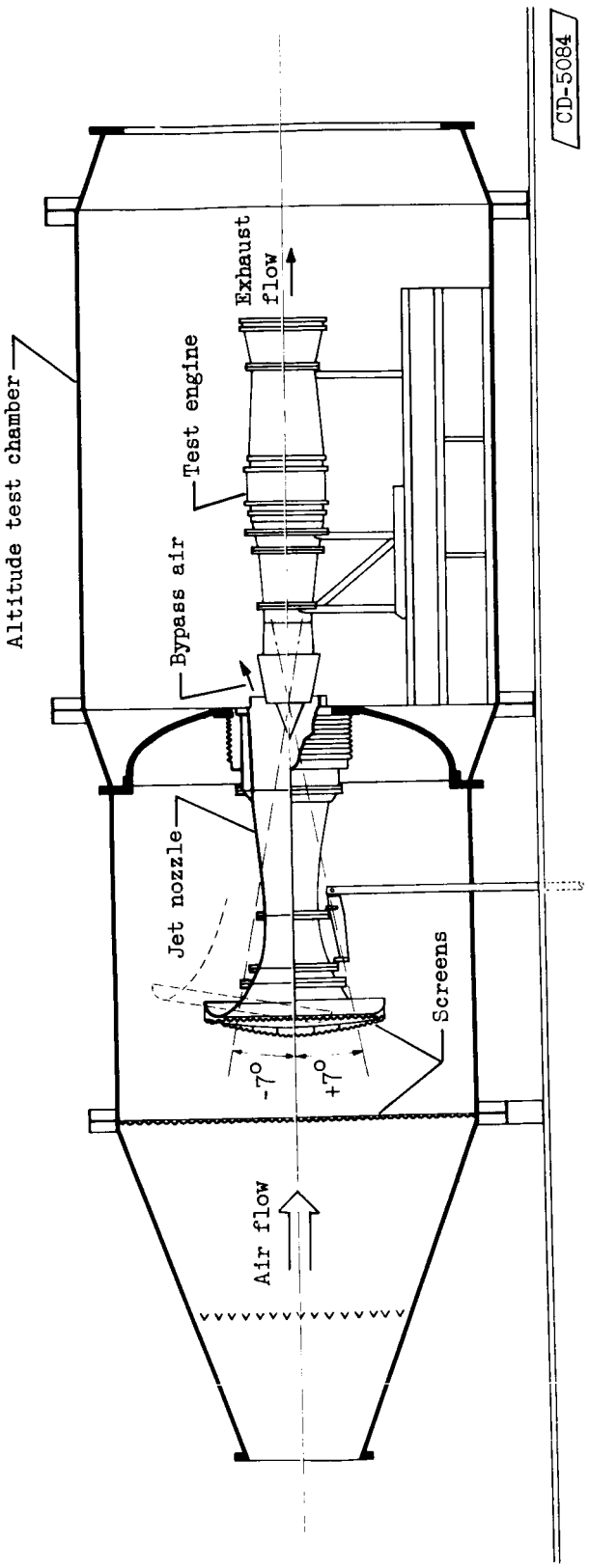

Figure 1. - Free-jet facility with engine installed showing positions of nozzle for simulation of angle of attack.

4058

4058

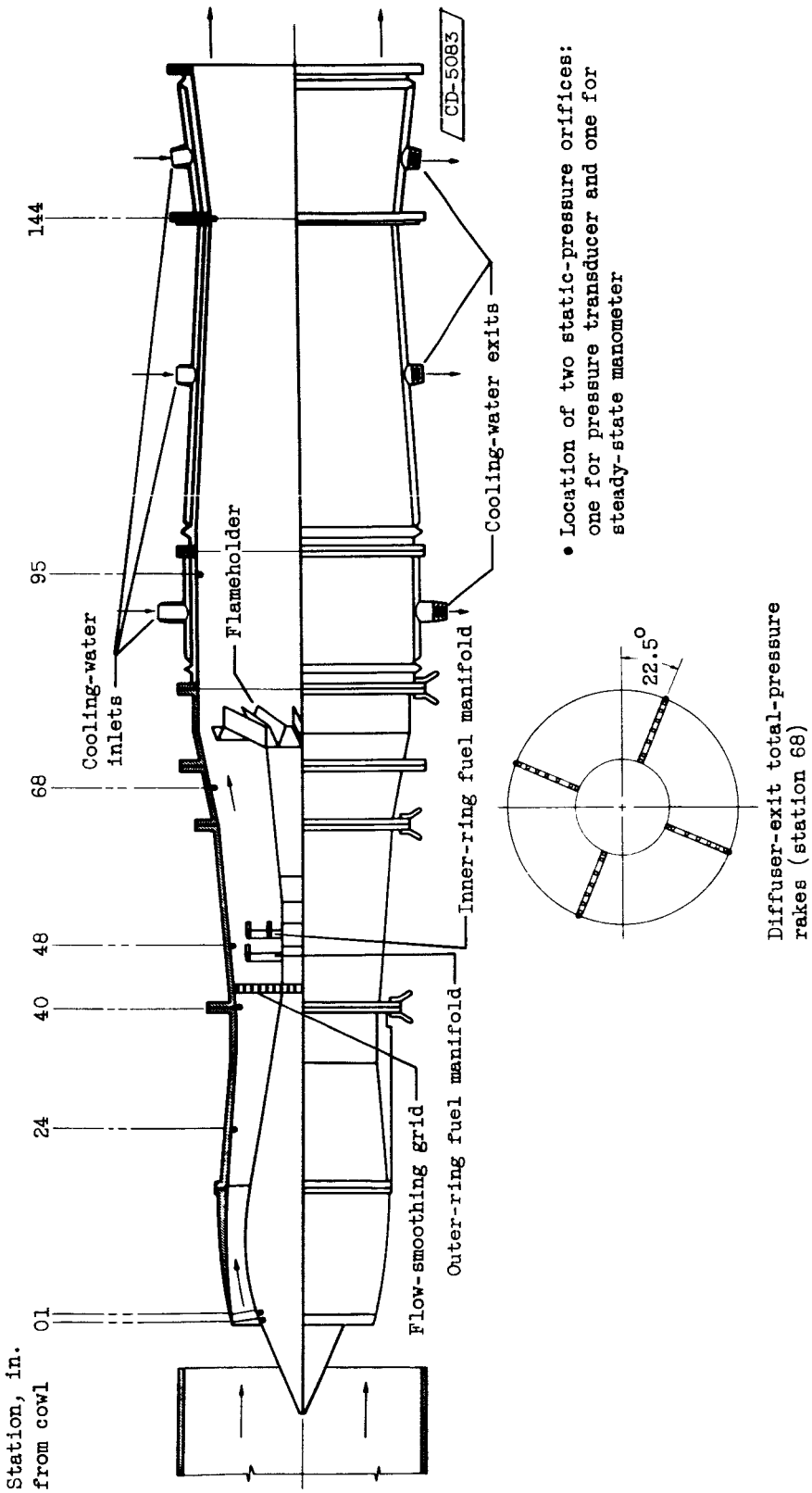

Figure 2. - 28-Inch ram-jet engine showing location of pressure instrumentation.

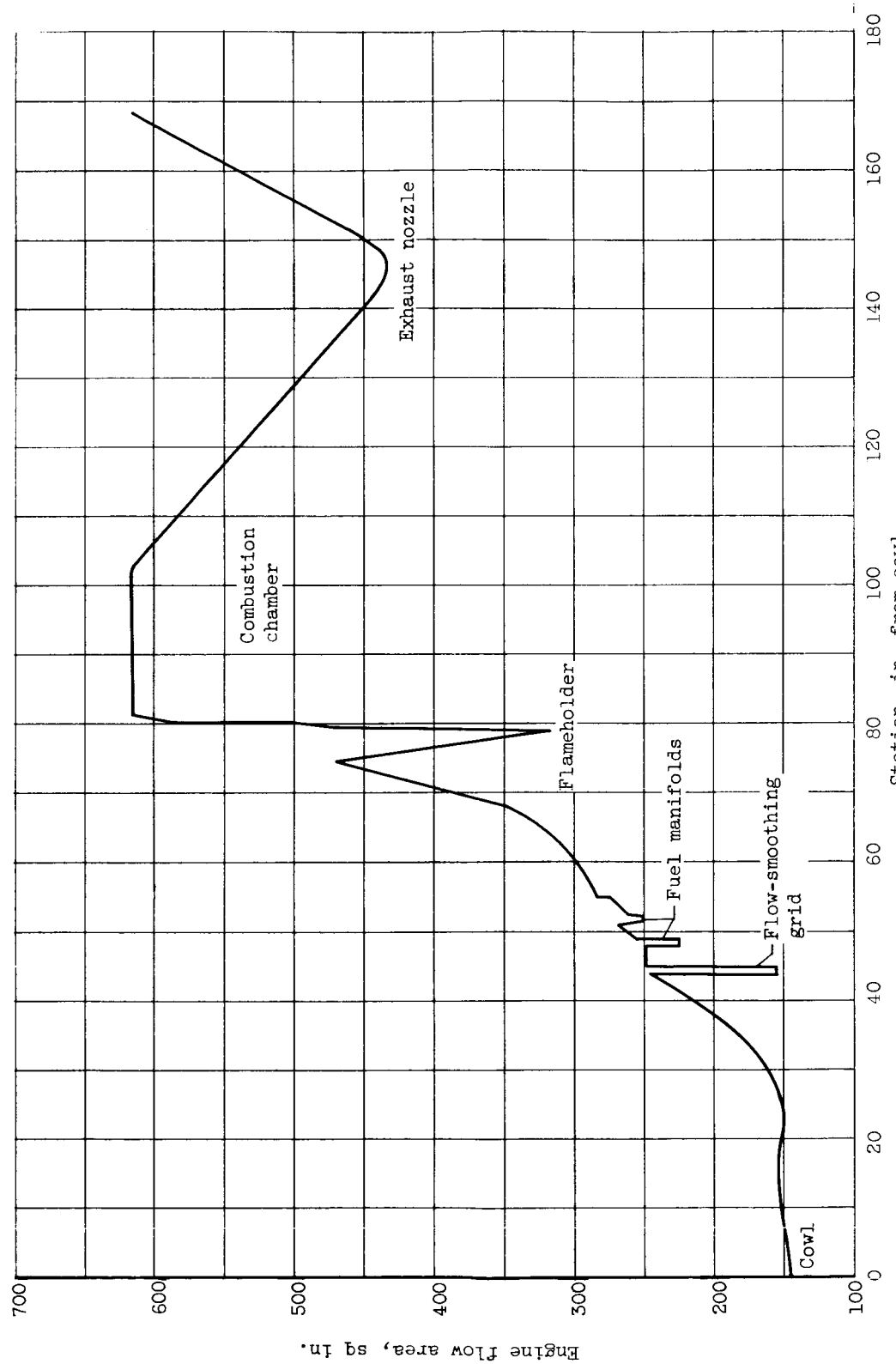

Figure 3. - Internal-flow area of 28-inch-diameter ram-jet engine.

4058

4058

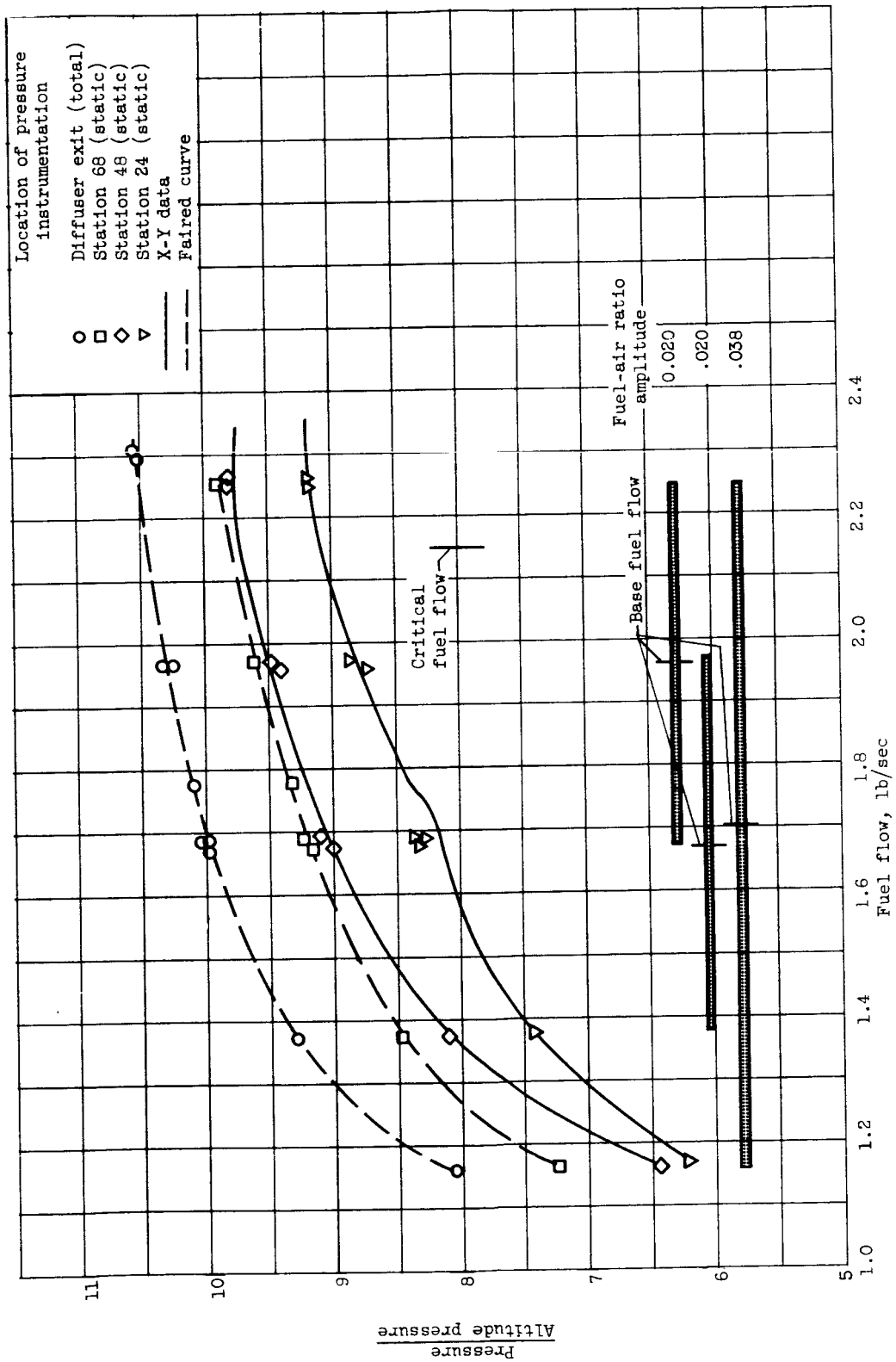

(a) Mach number, 2.50.

Figure 4. - Steady-state diffuser pressures and range of sinusoidal fuel flow disturbances at zero angle of attack. Altitude, 60,000 feet.

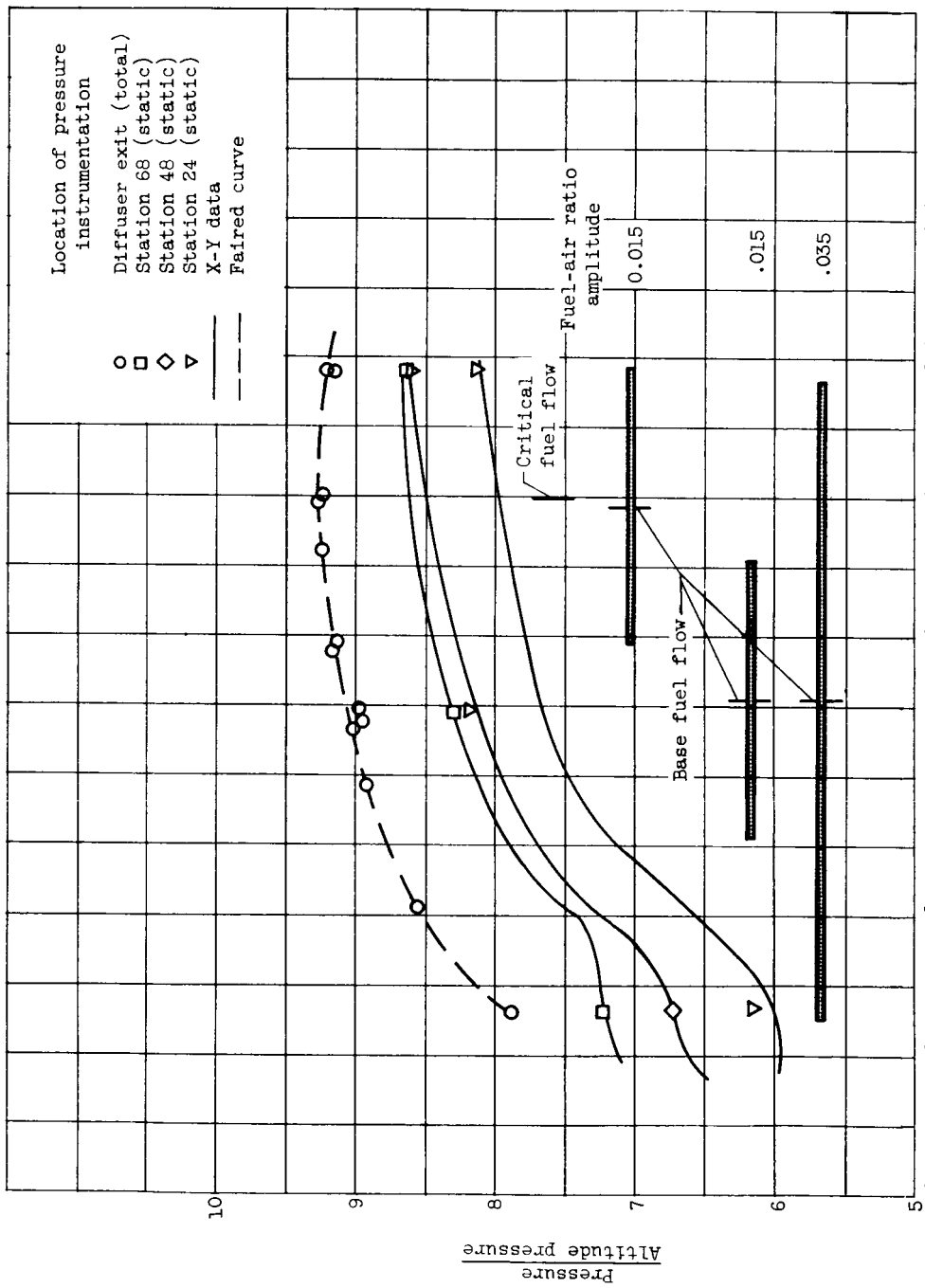

(b) Mach number, 2.35.

Figure 4. - Concluded. Steady-state diffuser pressures and range of sinusoidal fuel flow disturbances at zero angle of attack. Altitude, 60,000 feet.

4058

4058
CY-3

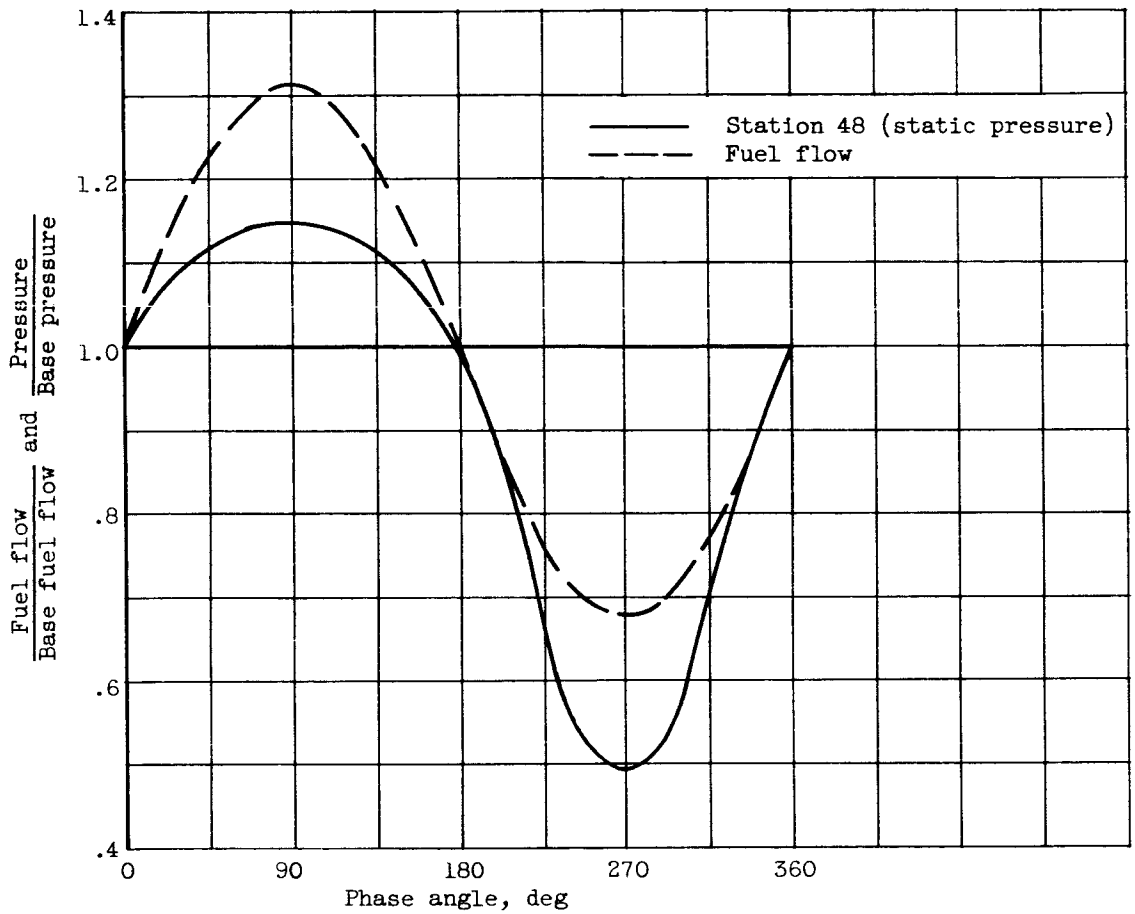

Figure 5. - Distortion of pressure response for 0.038 fuel-air ratio sinusoid amplitude variation determined from steady-state calibration. Mach number, 2.50.

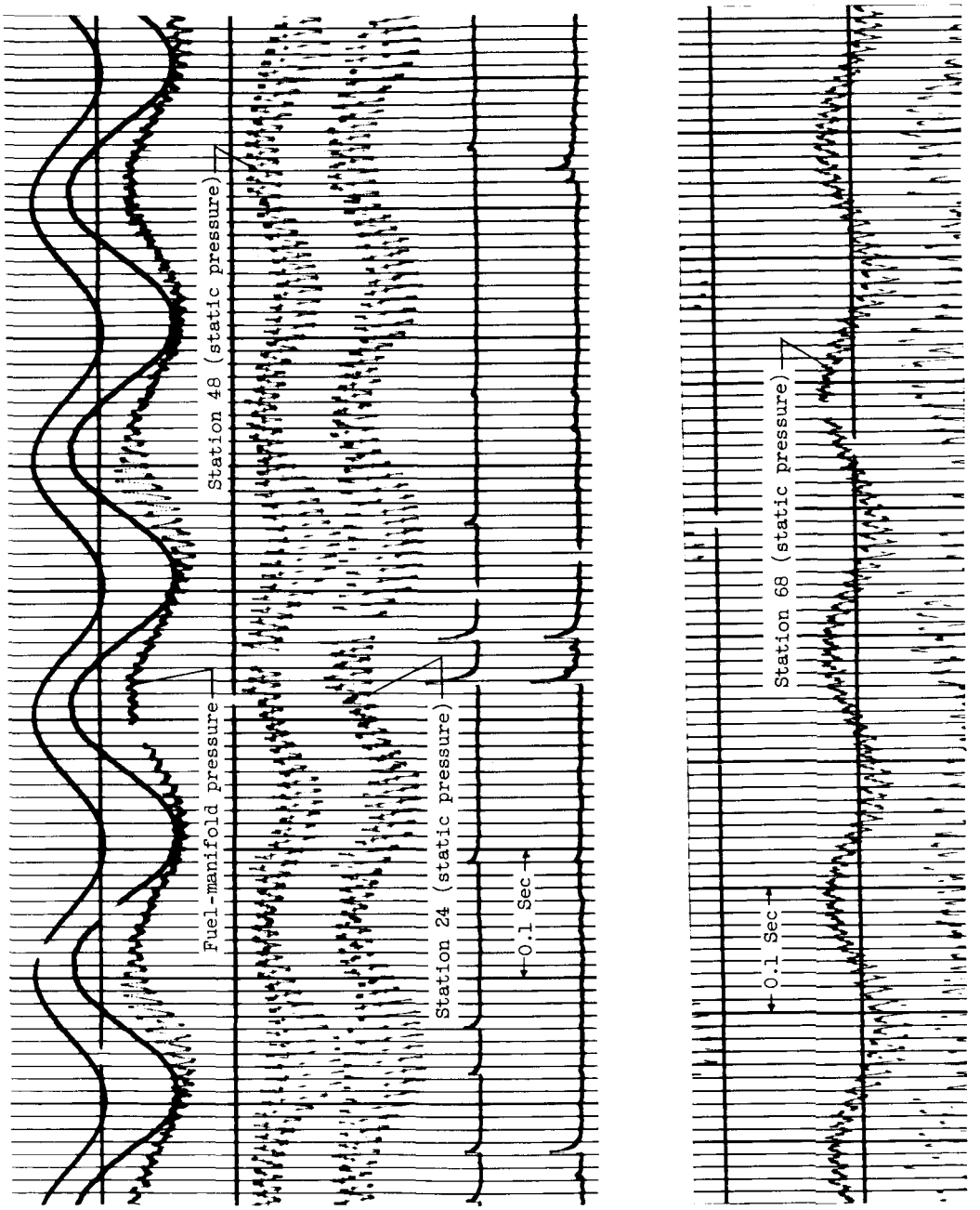

Figure 6. - Typical oscillogram of engine pressures. Mach number, 2.50; altitude, 60,000 feet; frequency, 5 cps.

4058

CY-3 back 4058

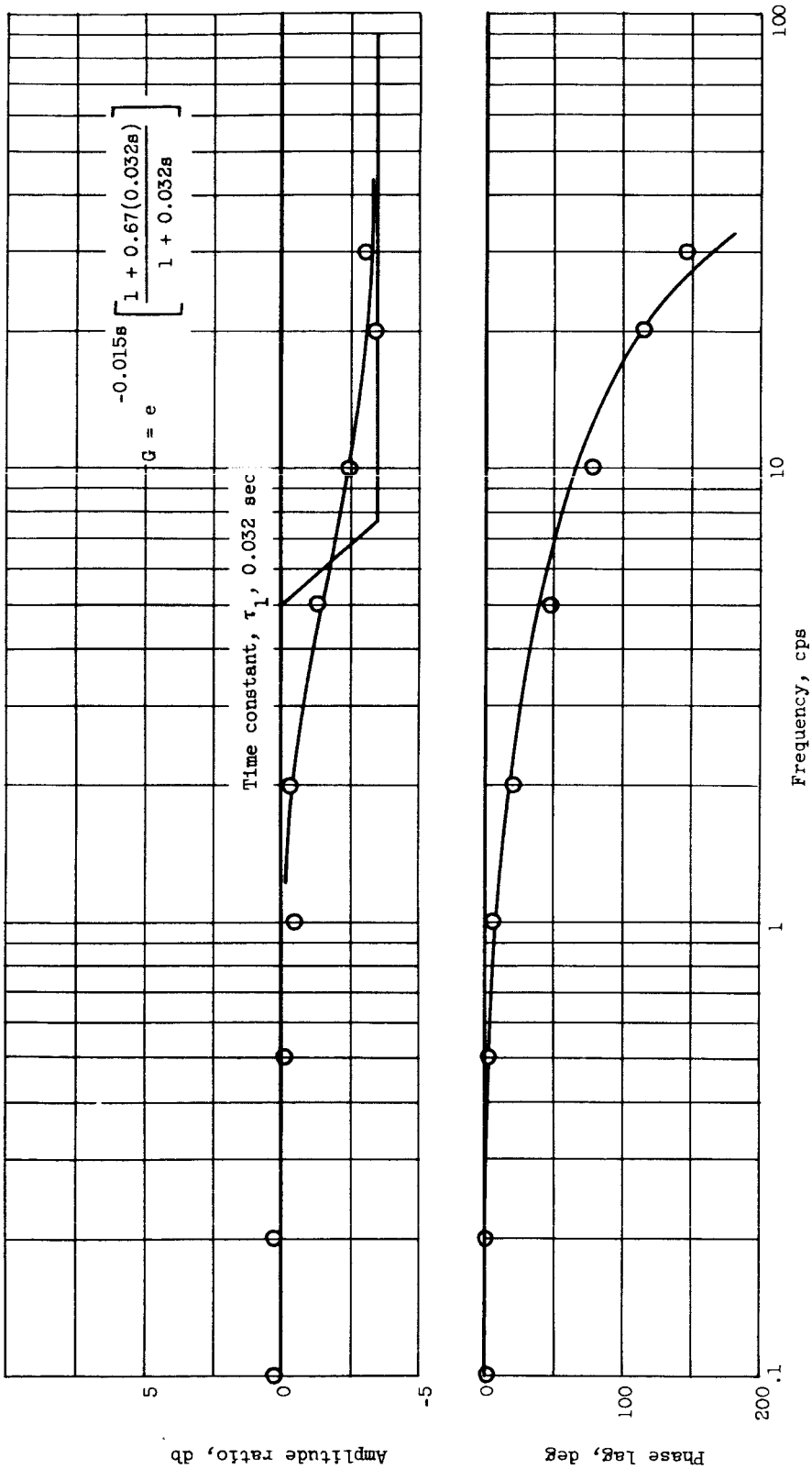

(a) Station 24; Mach number, 2.50; base diffuser-exit total-pressure ratio, 9.98; fuel-air ratio amplitude, 0.020.

Figure 7. - Frequency response to small-amplitude sinusoid at low base pressure recovery. Altitude, 60,000 feet; zero angle of attack.

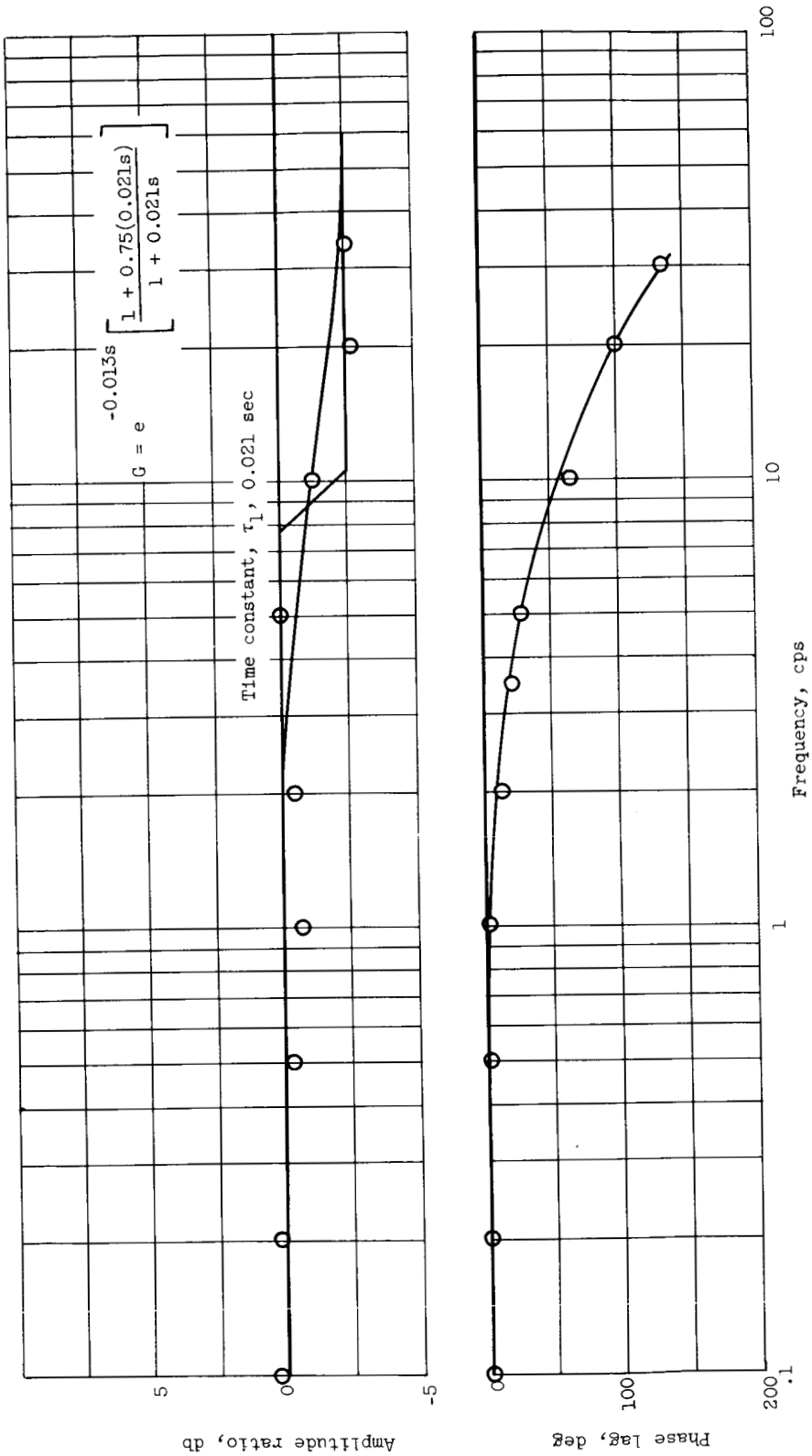

(b) Station 48; Mach number, 2.50; base diffuser-exit total-pressure ratio, 9.98; fuel-air ratio amplitude, 0.020.

Figure 7. - Continued. Frequency response to small-amplitude sinusoid at low base pressure recovery. Altitude, 60,000 feet; zero angle of attack.

4058

4058

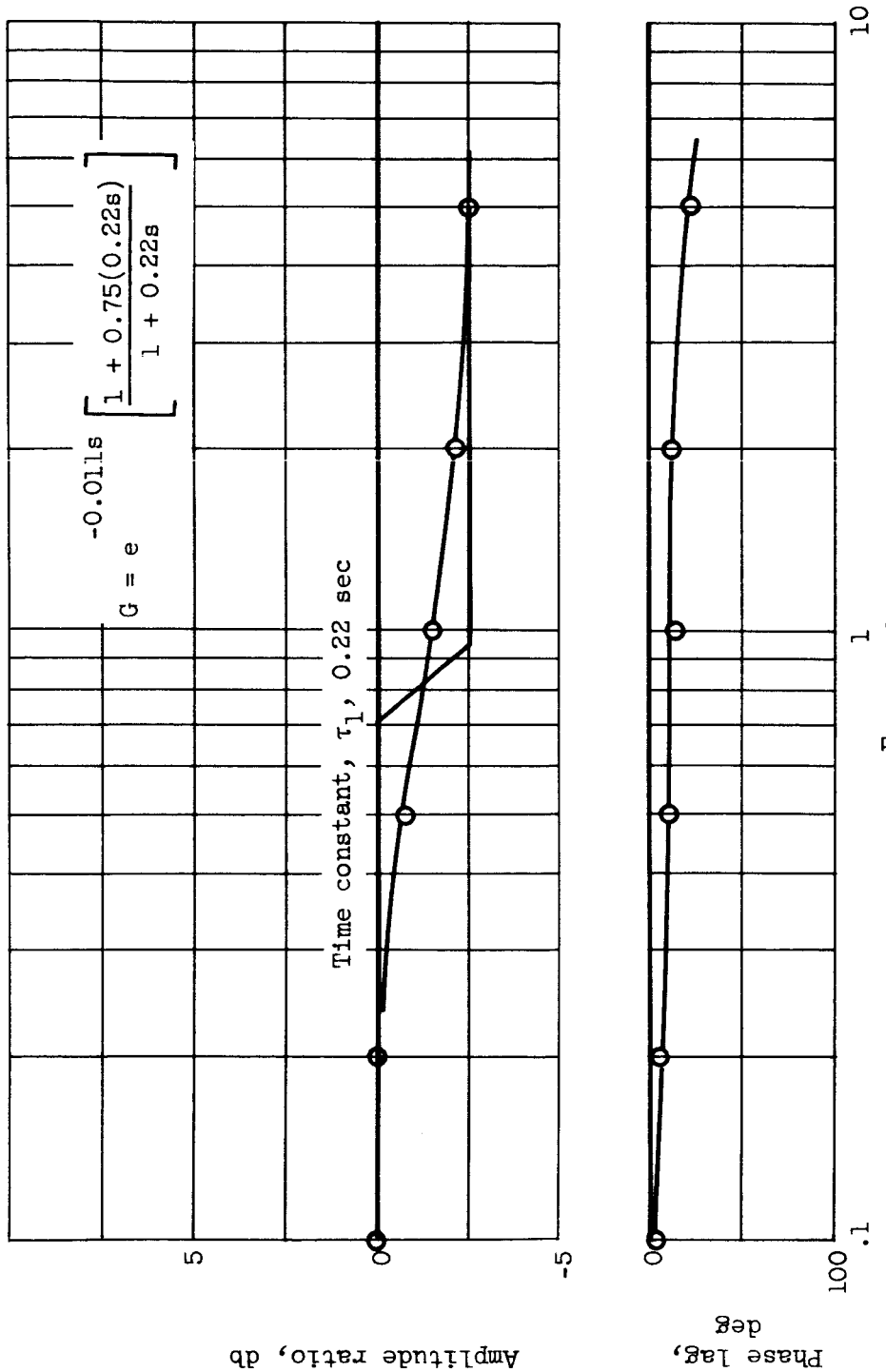

(c) Station 24; Mach number, 2.35; base diffuser-exit total-pressure ratio, 9.10; fuel-air ratio amplitude, 0.015.

Figure 7. - Continued. Frequency response to small-amplitude sinusoid at low base pressure recovery. Altitude, 60,000 feet; zero angle of attack.

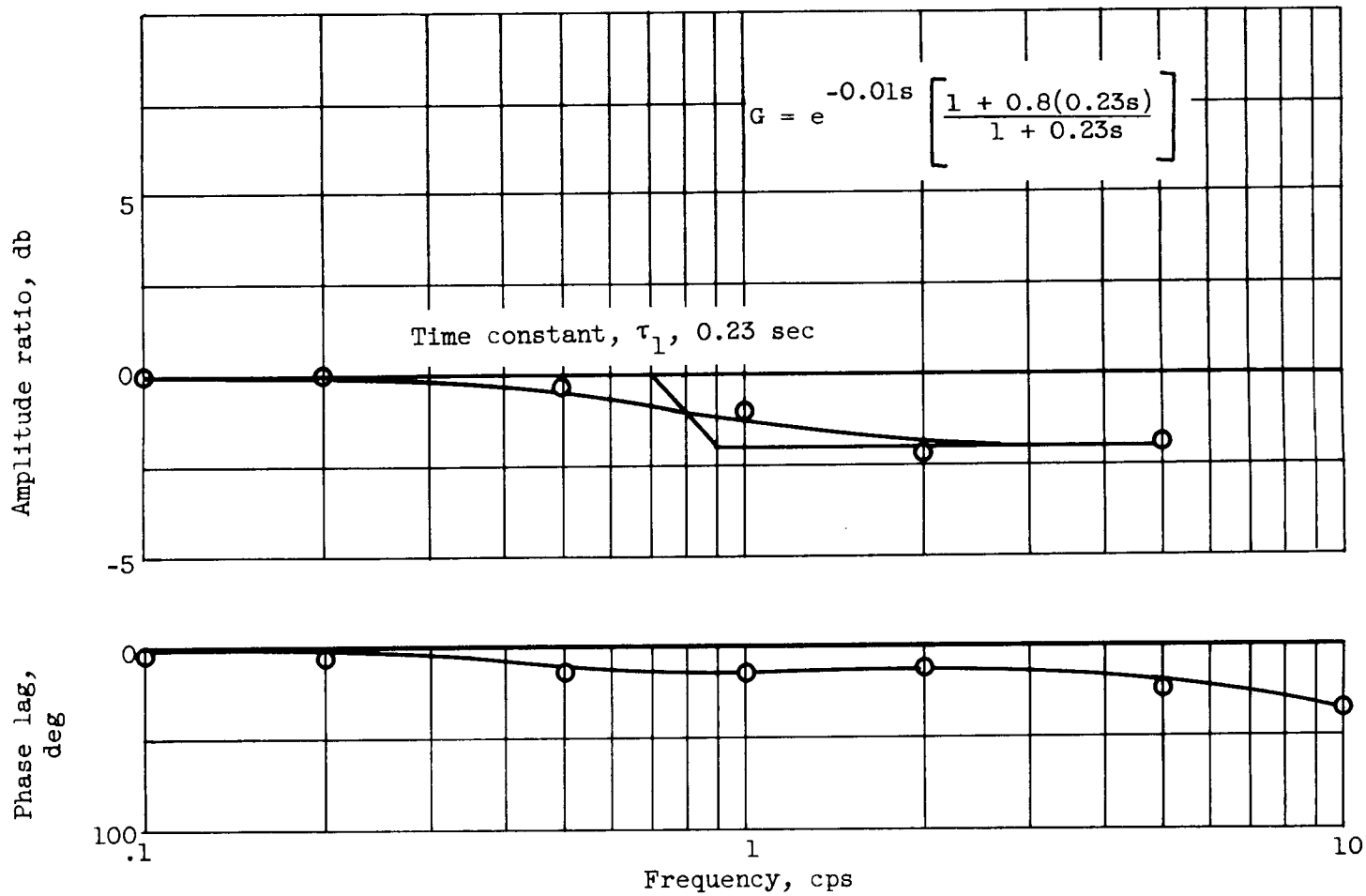

(d) Station 48; Mach number, 2.35; base diffuser-exit total-pressure ratio, 9.10; fuel-air ratio amplitude, 0.015.

Figure 7. - Concluded. Frequency response to small-amplitude sinusoid at low base pressure recovery. Altitude, 60,000 feet; zero angle of attack.

4058

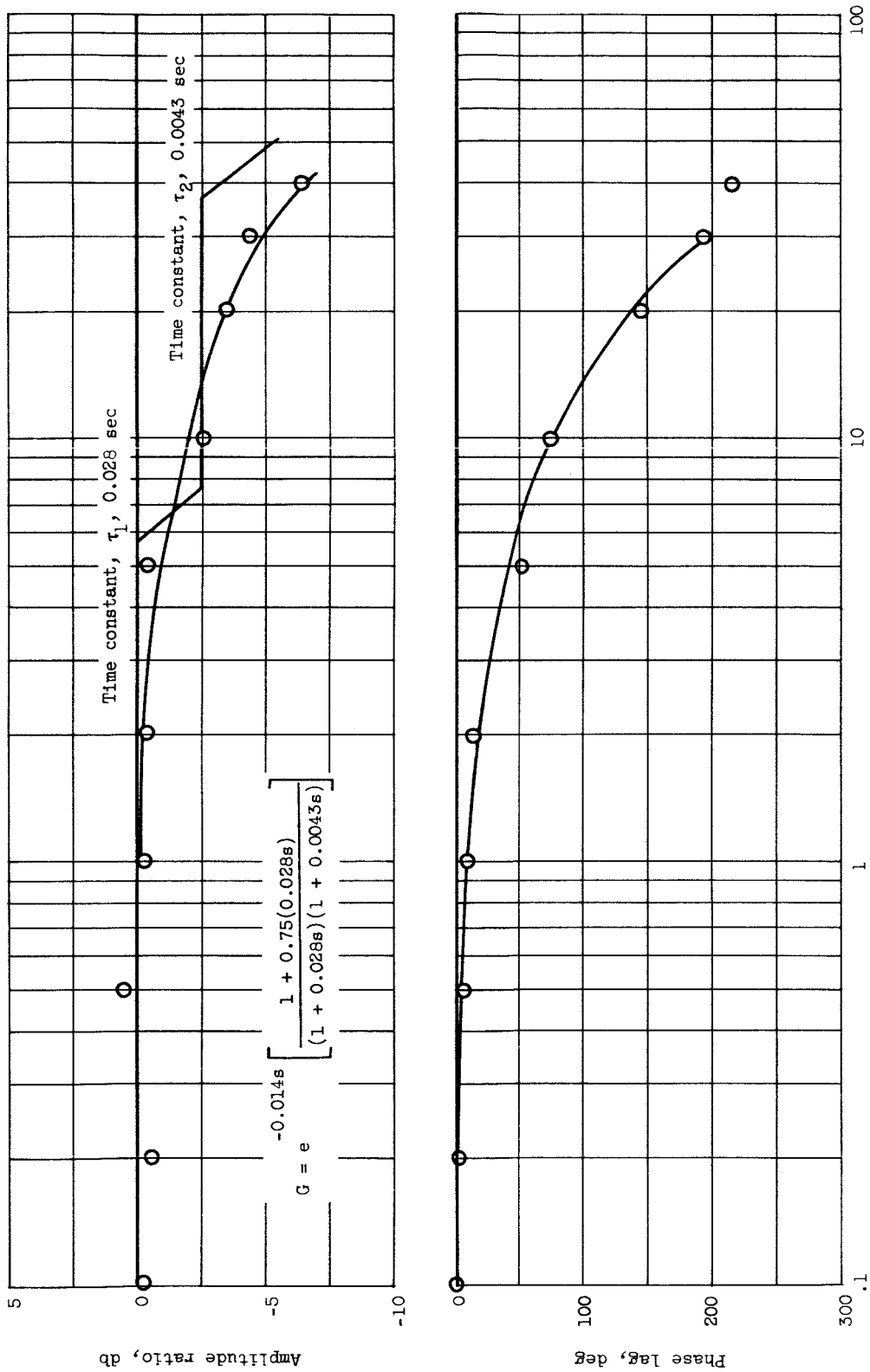

(a) Station 24; Mach number, 2.50; fuel-air ratio amplitude, 0.020; base diffuser-exit total-pressure ratio, 10.3.

Figure 8. - Frequency response to small-amplitude sinusoid at high base pressure recovery. Altitude, 60,000 feet; zero angle of attack.

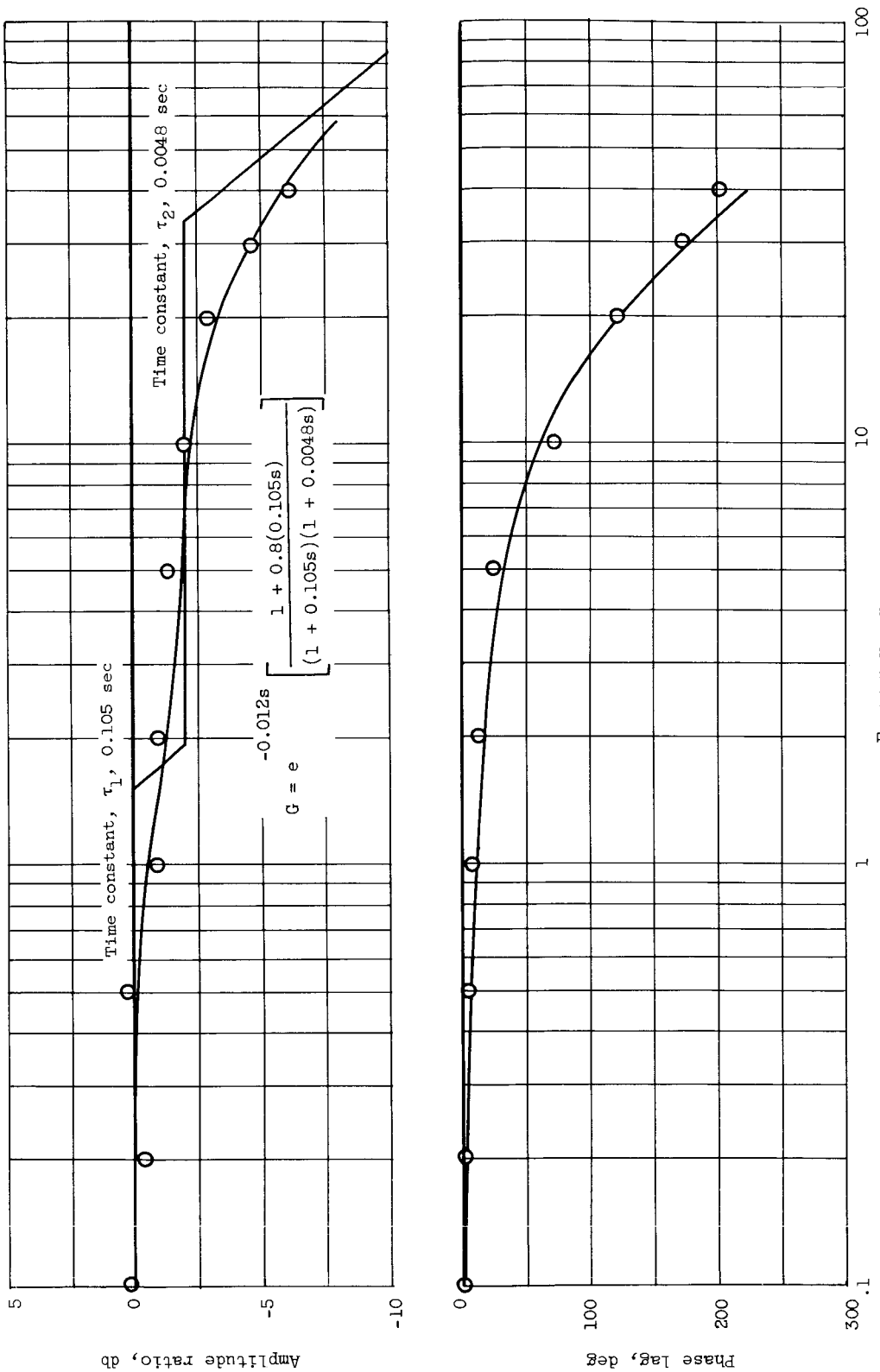

(b) Station 48; Mach number, 2.50; fuel-air ratio amplitude, 0.020; base diffuser-exit total-pressure ratio, 10.3.

Figure 8. - Continued. Frequency response to small-amplitude sinusoid at high base pressure recovery. Altitude, 60,000 feet; zero angle of attack.

4058

CY-4 4058

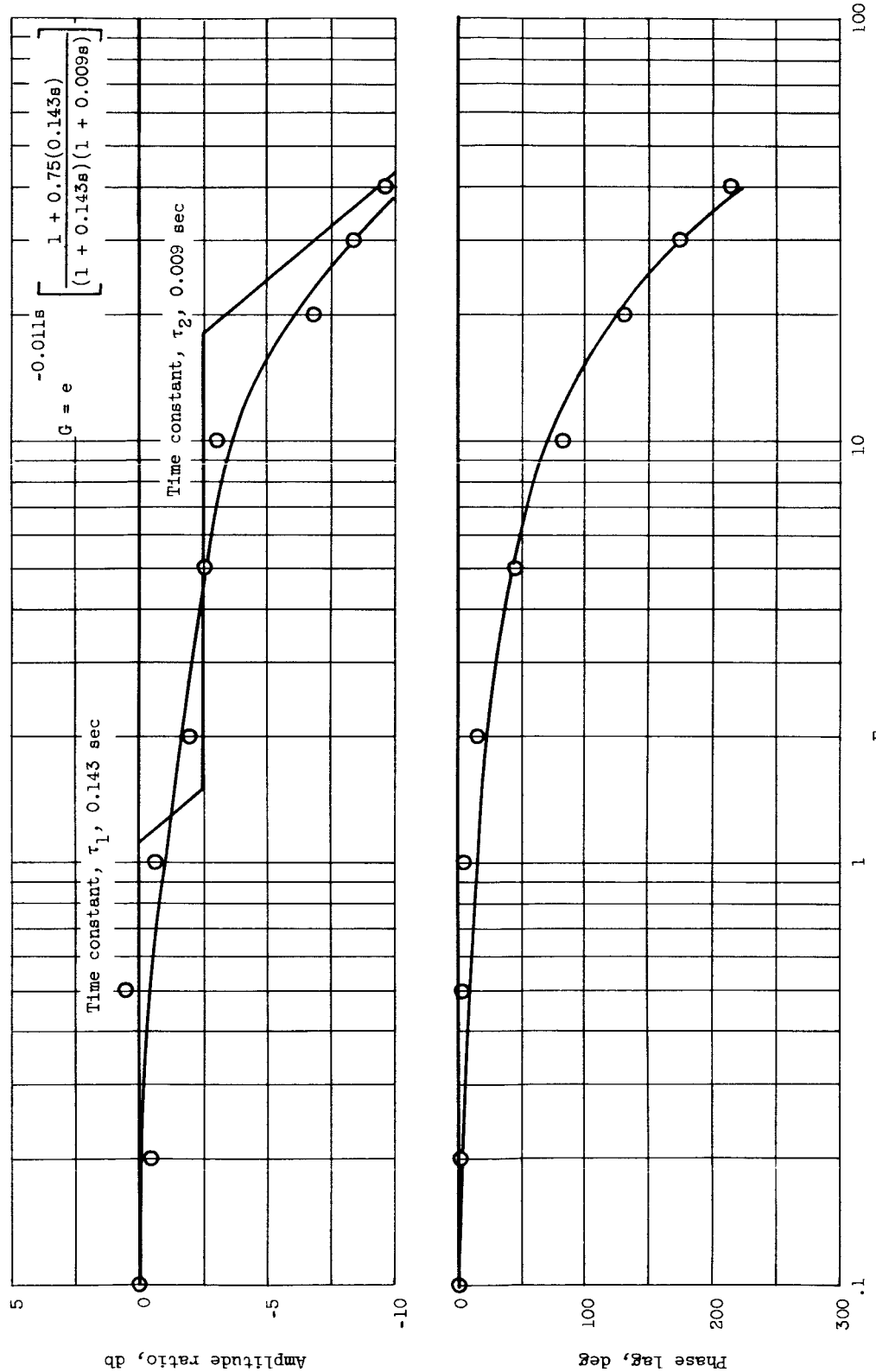

(c) Station 68; Mach number, 2.50; fuel-air ratio amplitude, 0.020; base diffuser-exit total-pressure ratio, 10.3.

Figure 8. - Continued. Frequency response to small-amplitude sinusoid at high base pressure recovery. Altitude, 60,000 feet; zero angle of attack.

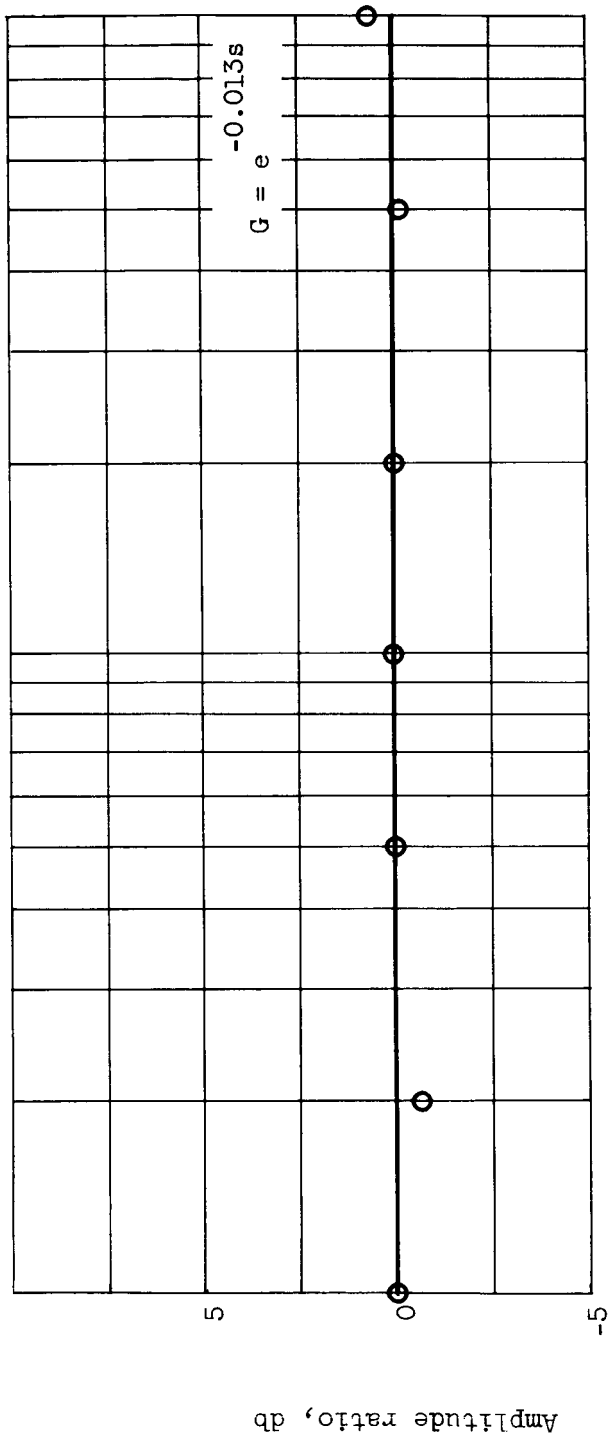

(d) Station 24; Mach number, 2.35; fuel-air ratio amplitude, 0.015; base diffuser-exit total-pressure ratio, 9.26.

Figure 8. - Continued. Frequency response to small-amplitude sinusoid at high base pressure recovery. Altitude, 60,000 feet; zero angle of attack.

4058

CY-4 back 4058

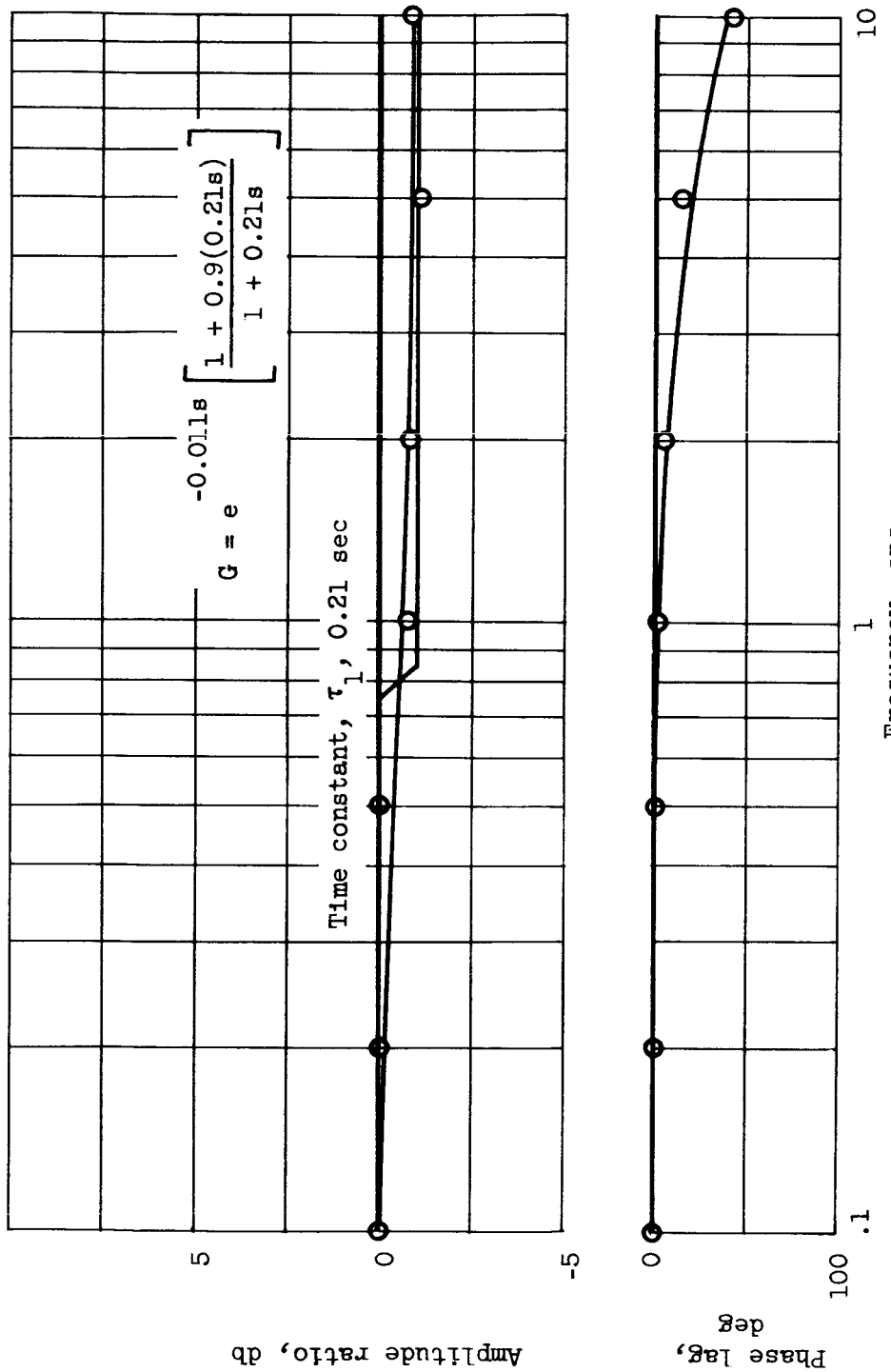

(e) Station 48; Mach number, 2.35; fuel-air ratio amplitude, 0.015; base diffuser-exit total-pressure ratio, 9.26.

Figure 8. - Continued. Frequency response to small-amplitude sinusoid at high base pressure recovery. Altitude, 60,000 feet; zero angle of attack.

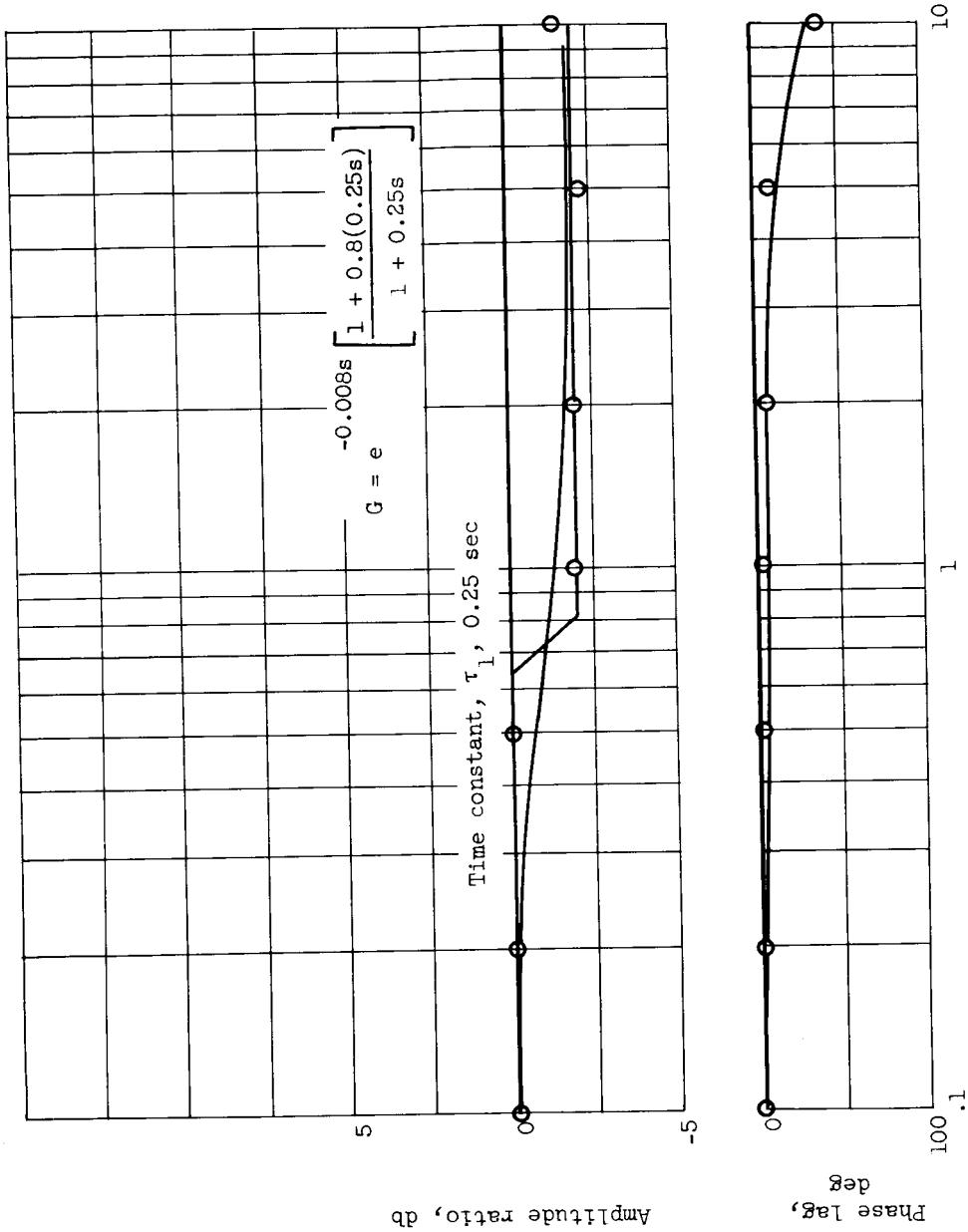

(f) Station 68; Mach number, 2.35; fuel-air ratio amplitude, 0.015; base diffuser-exit total-pressure ratio, 9.26.

Figure 8. - Concluded. Frequency response to small-amplitude sinusoid at high base pressure recovery. Altitude, 60,000 feet; zero angle of attack.

4058

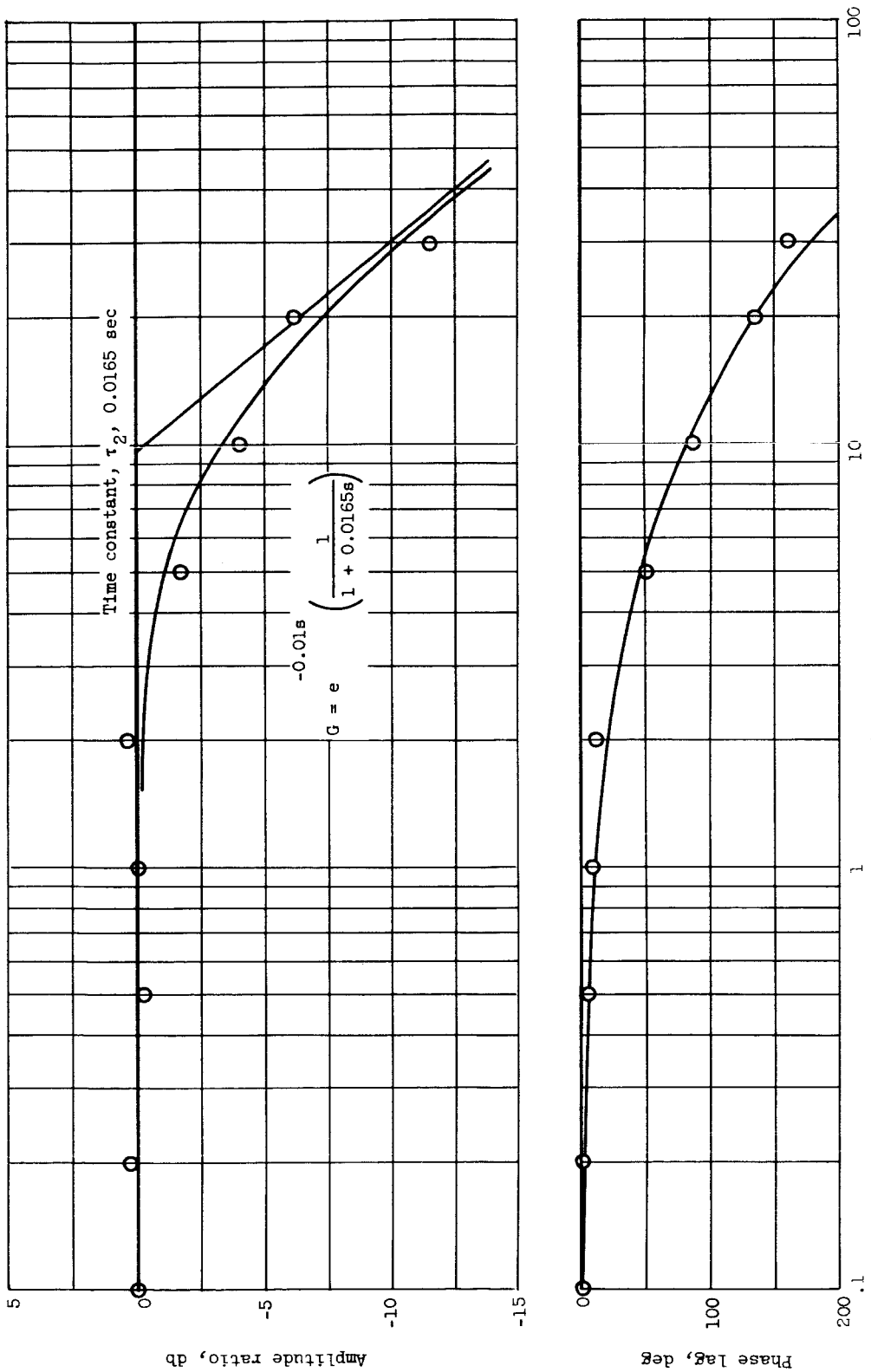

(a) Station 24; Mach number, 2.50; fuel-air ratio amplitude, 0.038; base diffuser-exit total-pressure ratio, 10.0.

Figure 9. - Frequency response to large-amplitude fuel sinusoid at low base pressure recovery. Altitude, 60,000 feet; zero angle of attack.

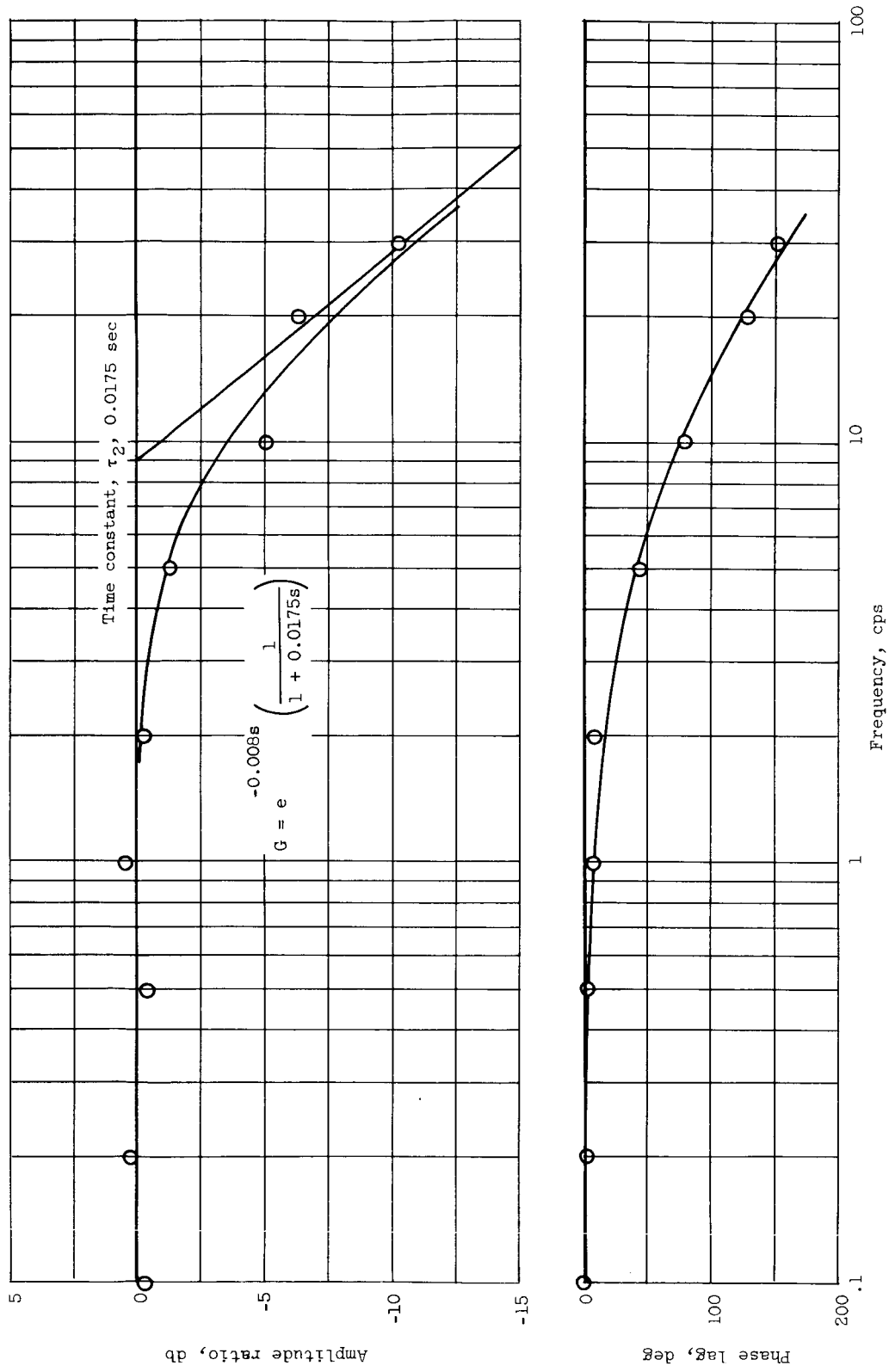

(b) Station 48; Mach number, 2.50; fuel-air ratio amplitude, 0.038; base diffuser-exit total-pressure ratio, 10.0.

Figure 9. - Continued. Frequency response to large-amplitude fuel sinusoid at low base pressure recovery. Altitude, 60,000 feet; zero angle of attack.

4058

4058

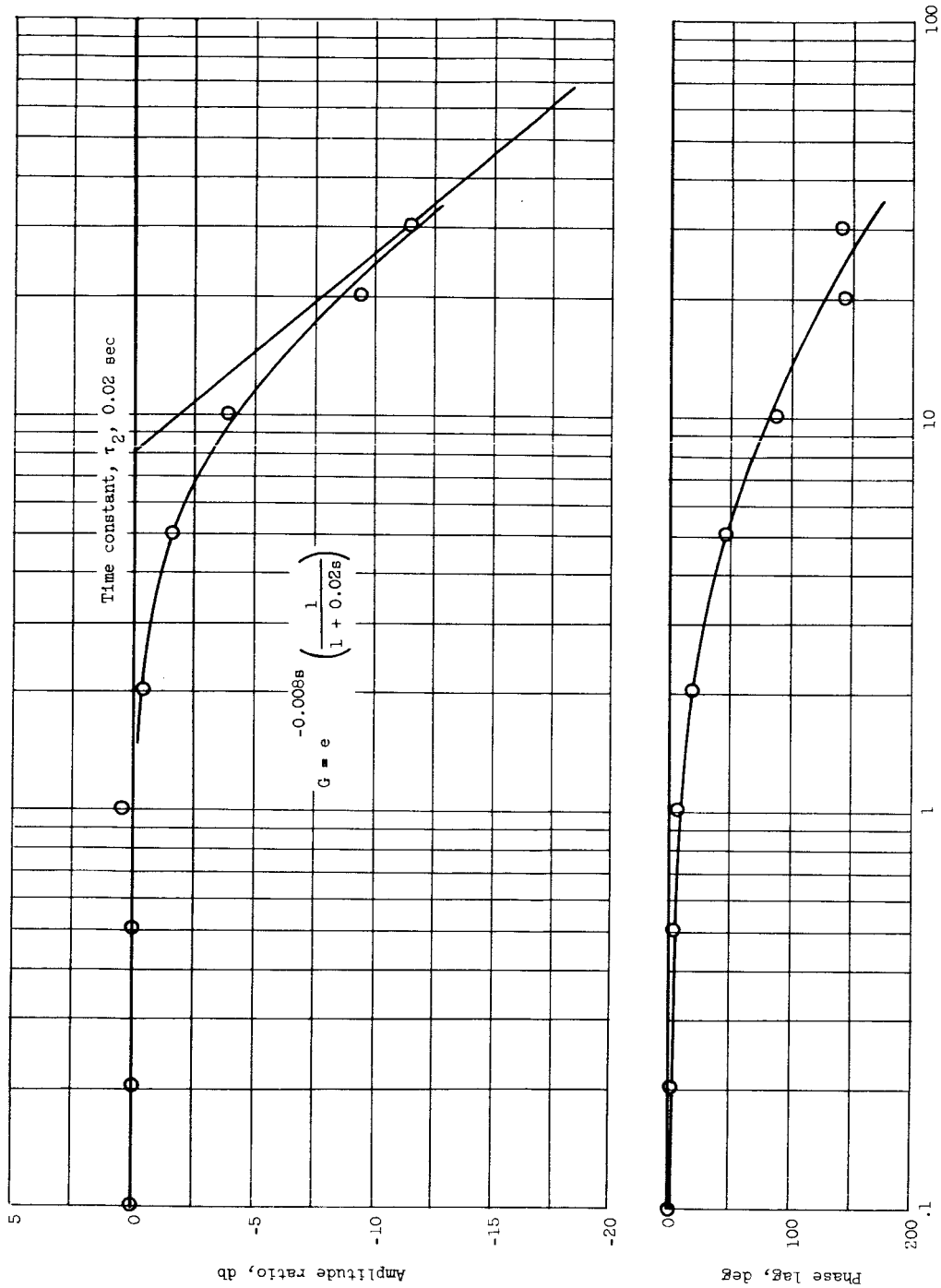

(c) Station 68; Mach number, 2.50; fuel-air ratio amplitude, 0.038; base diffuser-exit total-pressure ratio, 10.0.

Figure 9. - Continued. Frequency response to large-amplitude fuel sinusoid at low base pressure recovery. Altitude, 60,000 feet; zero angle of attack.

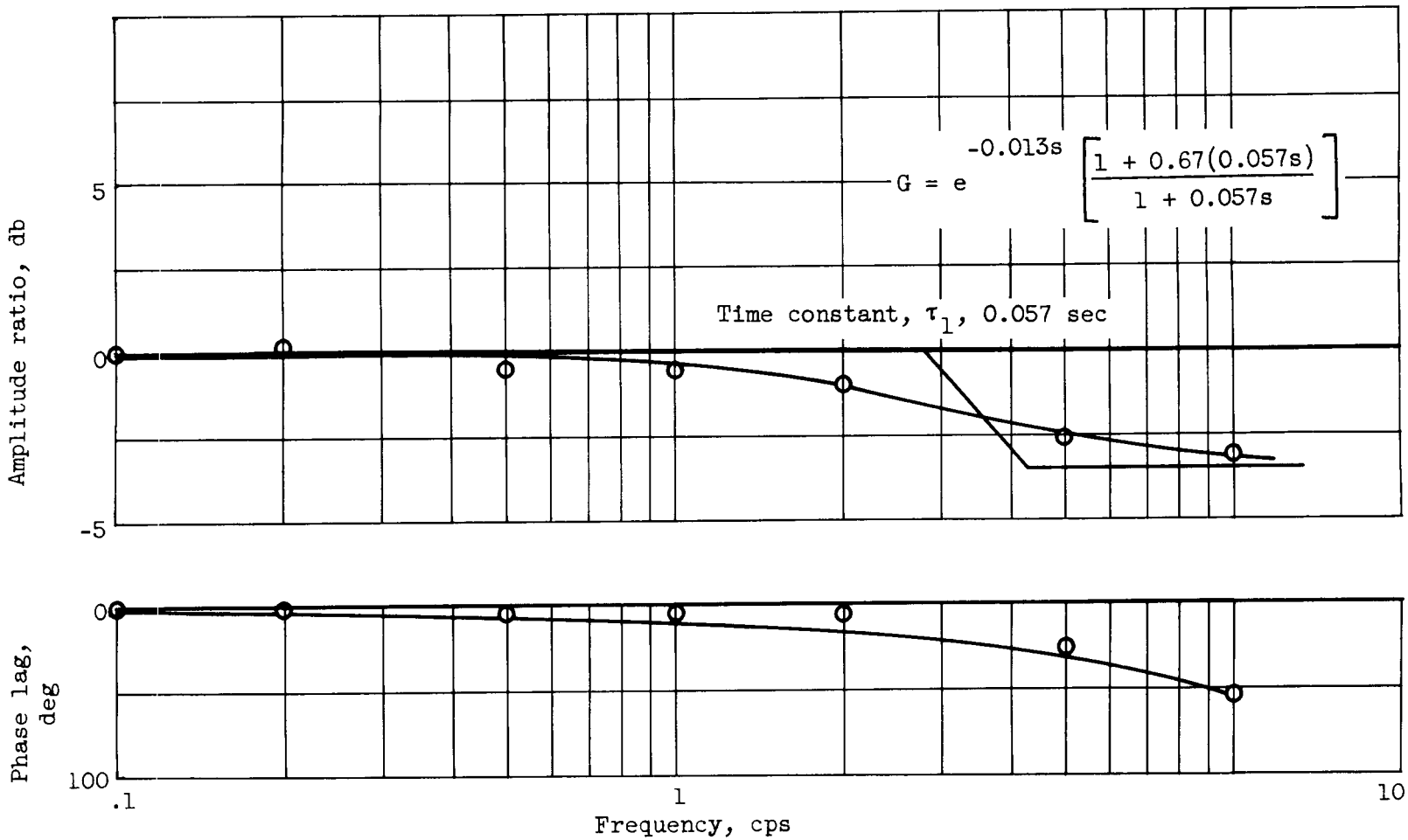

(d) Station 24; Mach number, 2.35; fuel-air ratio amplitude, 0.035; base diffuser-exit total-pressure ratio, 9.05.

Figure 9. - Continued. Frequency response to large-amplitude fuel sinusoid at low base pressure recovery. Altitude, 60,000 feet; zero angle of attack.

CONFIDENTIAL

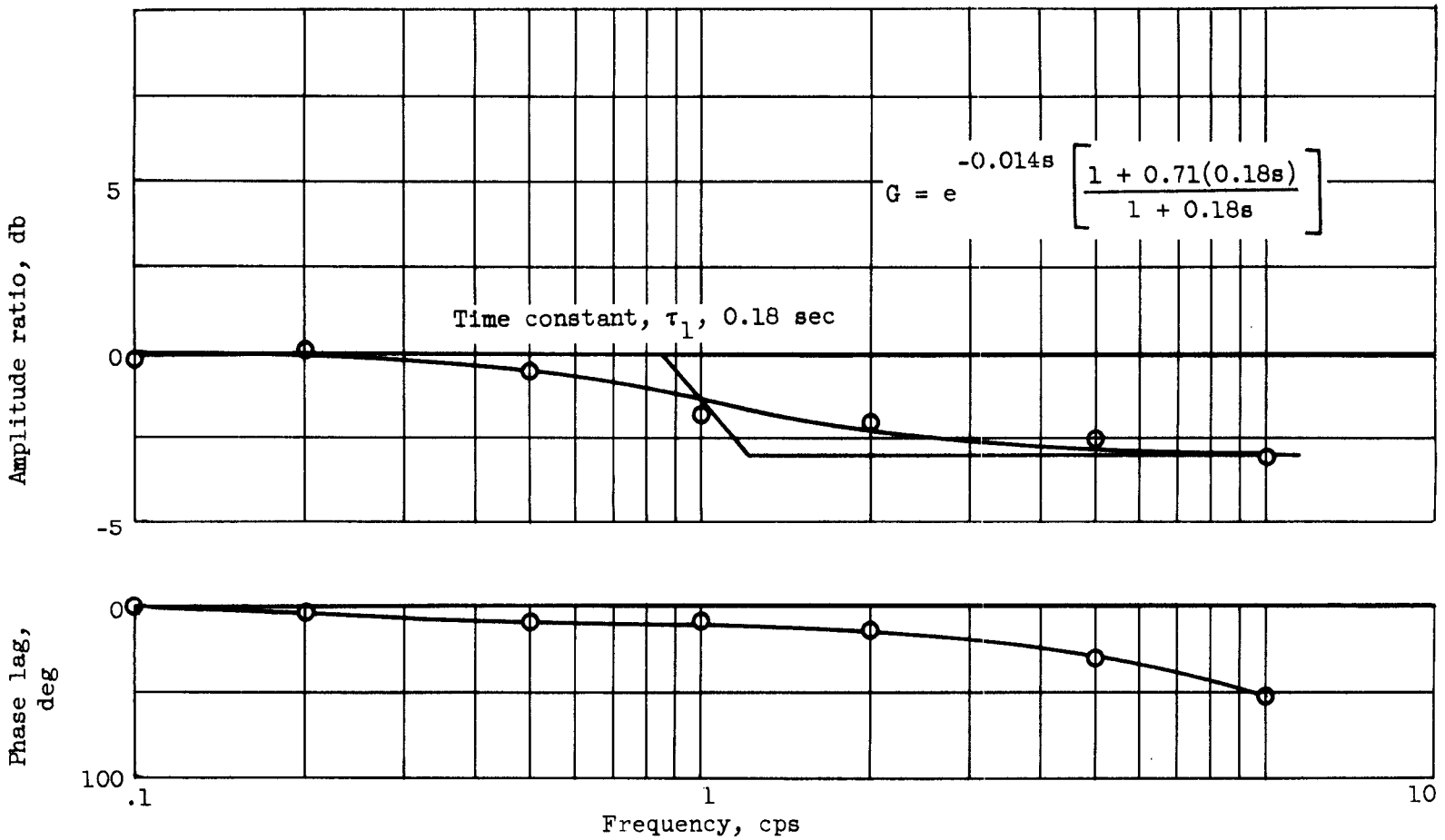

(e) Station 48; Mach number, 2.35; fuel-air ratio amplitude, 0.035; base diffuser-exit total-pressure ratio, 9.05.

Figure 9. - Continued. Frequency response to large-amplitude fuel sinusoid at low base pressure recovery. Altitude, 60,000 feet; zero angle of attack.

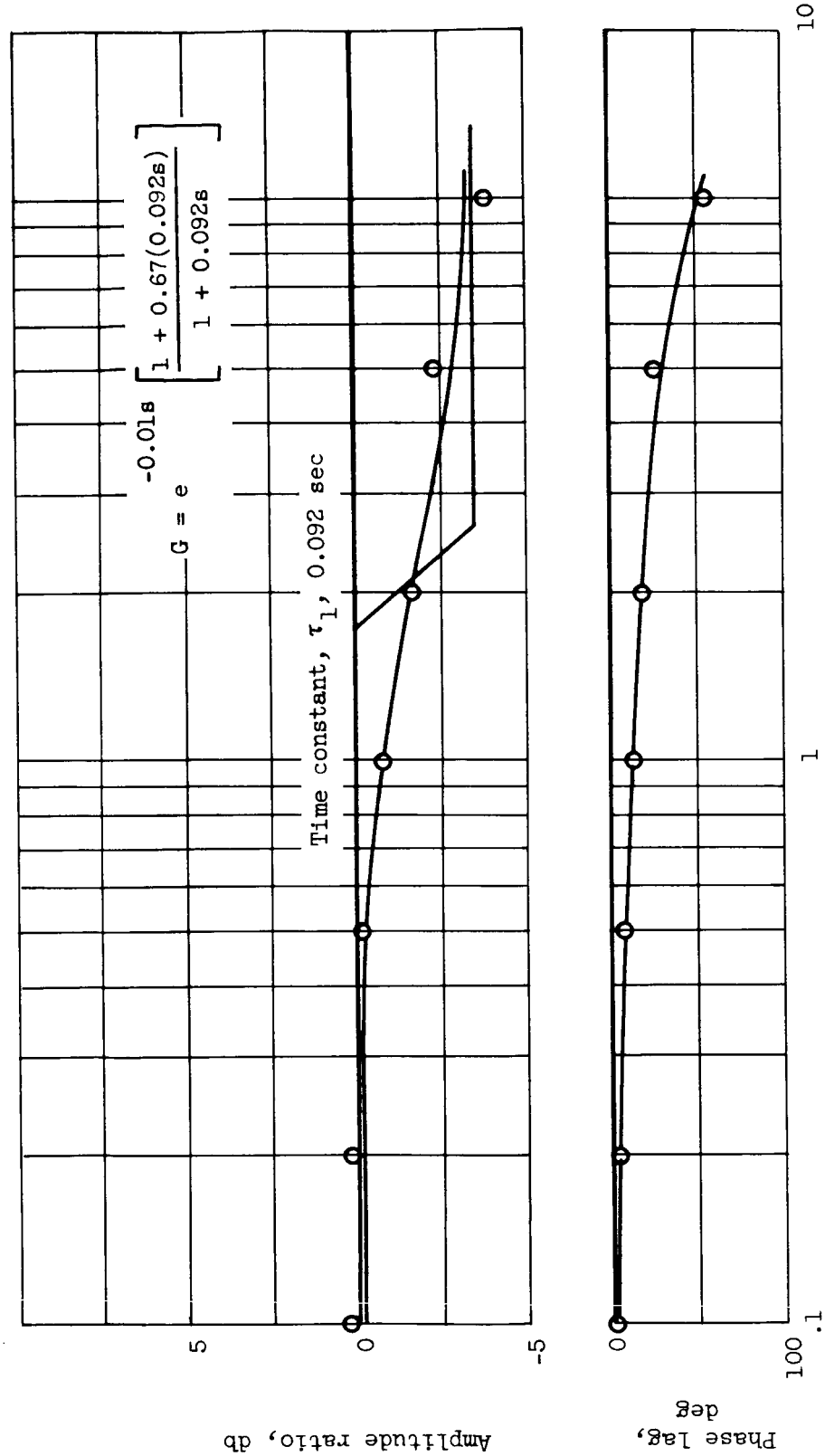

(f) Station 68; Mach number, 2.35; fuel-air ratio amplitude, 0.035; base diffuser-exit total-pressure ratio, 9.05.

Figure 9. - Concluded. Frequency response to large-amplitude fuel sinusoid at low base pressure recovery. Altitude, 60,000 feet; zero angle of attack.

4058

CY-5 back 4058

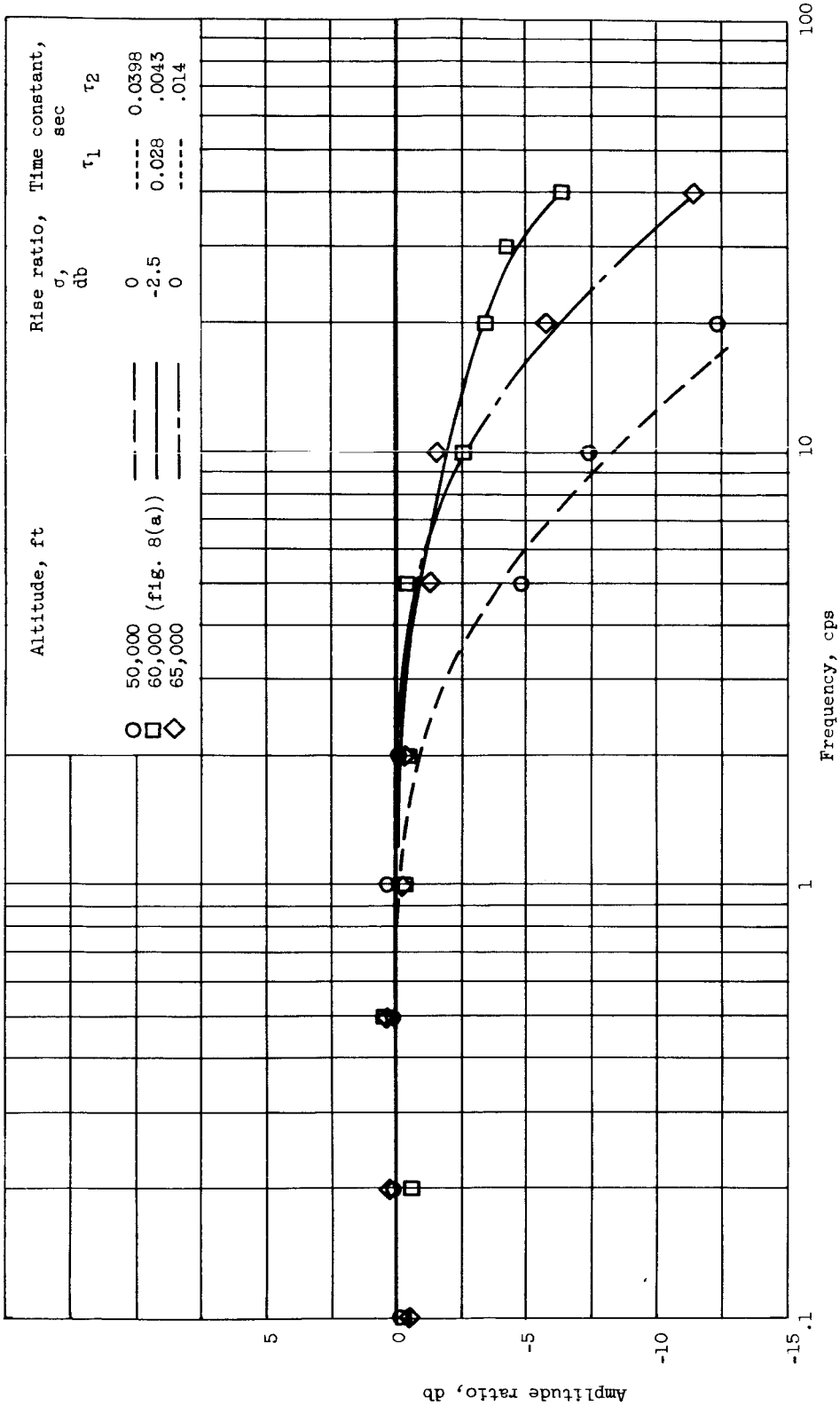

(a) Station 24.

Figure 10. - Effect of altitude on frequency response to sinusoidal fuel variation. Mach number, 2.50; base diffuser-exit total-pressure ratio, 10.3; fuel-air ratio amplitude, 0.020.

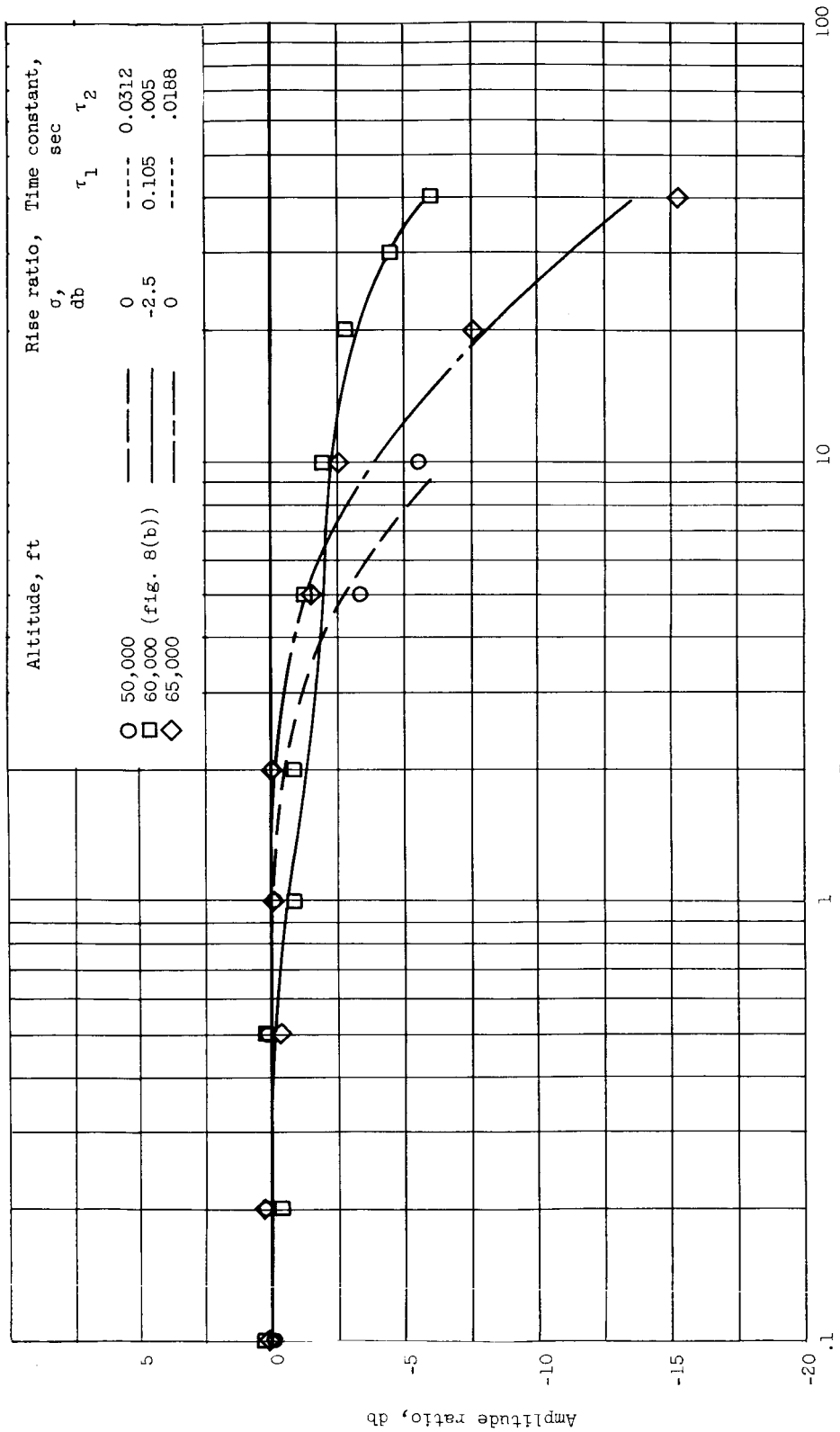

(b) Station 48.

Figure 10. - Continued. Effect of altitude on frequency response to sinusoidal fuel variation. Mach number, 2.50; base diffuser-exit total-pressure ratio, 10.3; fuel-air ratio amplitude, 0.020.

4058

4058

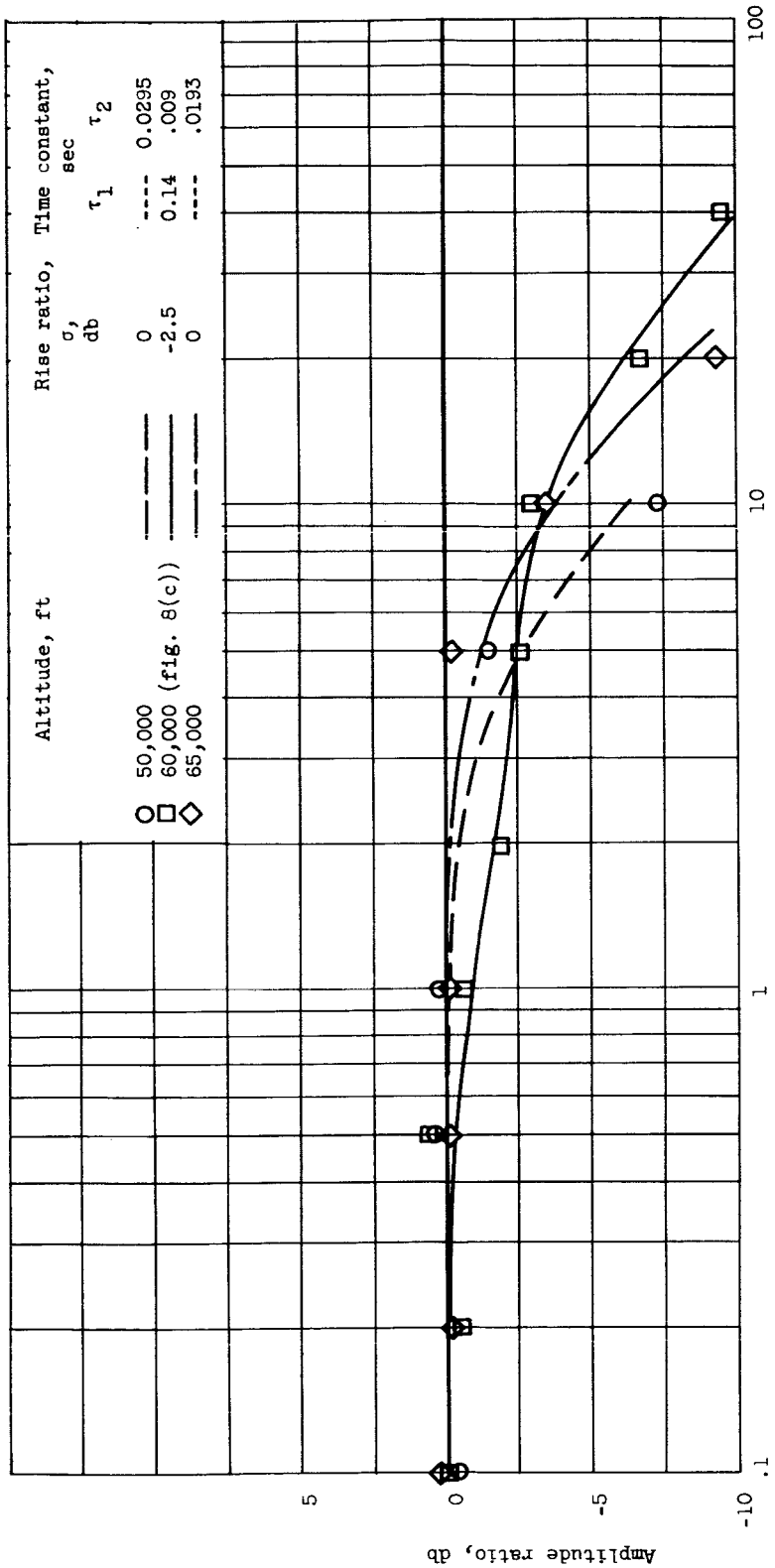

(c) Station 68.

Figure 10. - Concluded. Effect of altitude on frequency response to sinusoidal fuel variation. Mach number, 2.50; base diffuser-exit total-pressure ratio, 10.3; fuel-air ratio amplitude, 0.020.

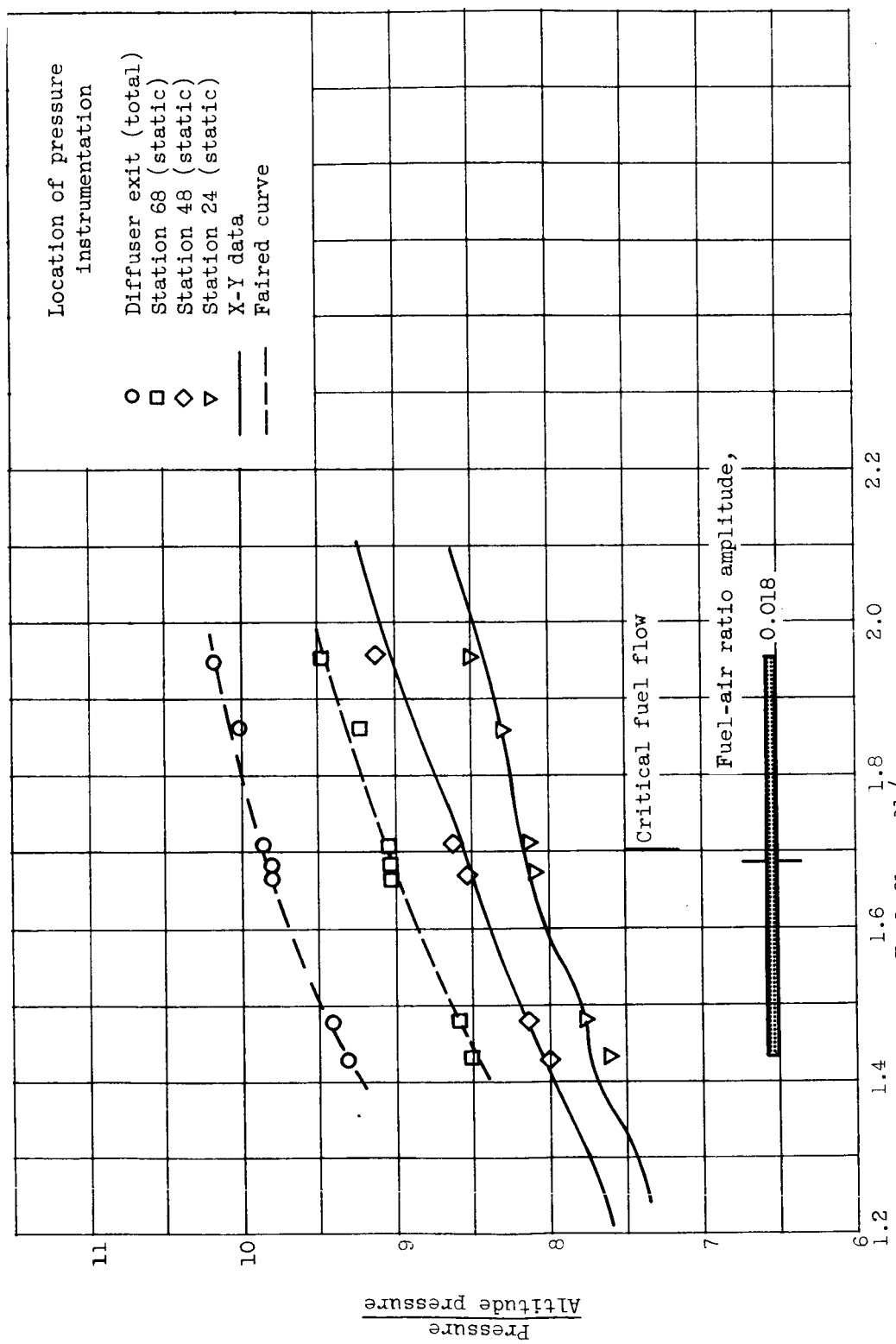

Figure 11. - Steady-state diffuser pressures and range of sinusoidal fuel flow disturbances at an angle of attack of +7°. Mach number, 2.50; altitude, 60,000 feet.

4058

4058

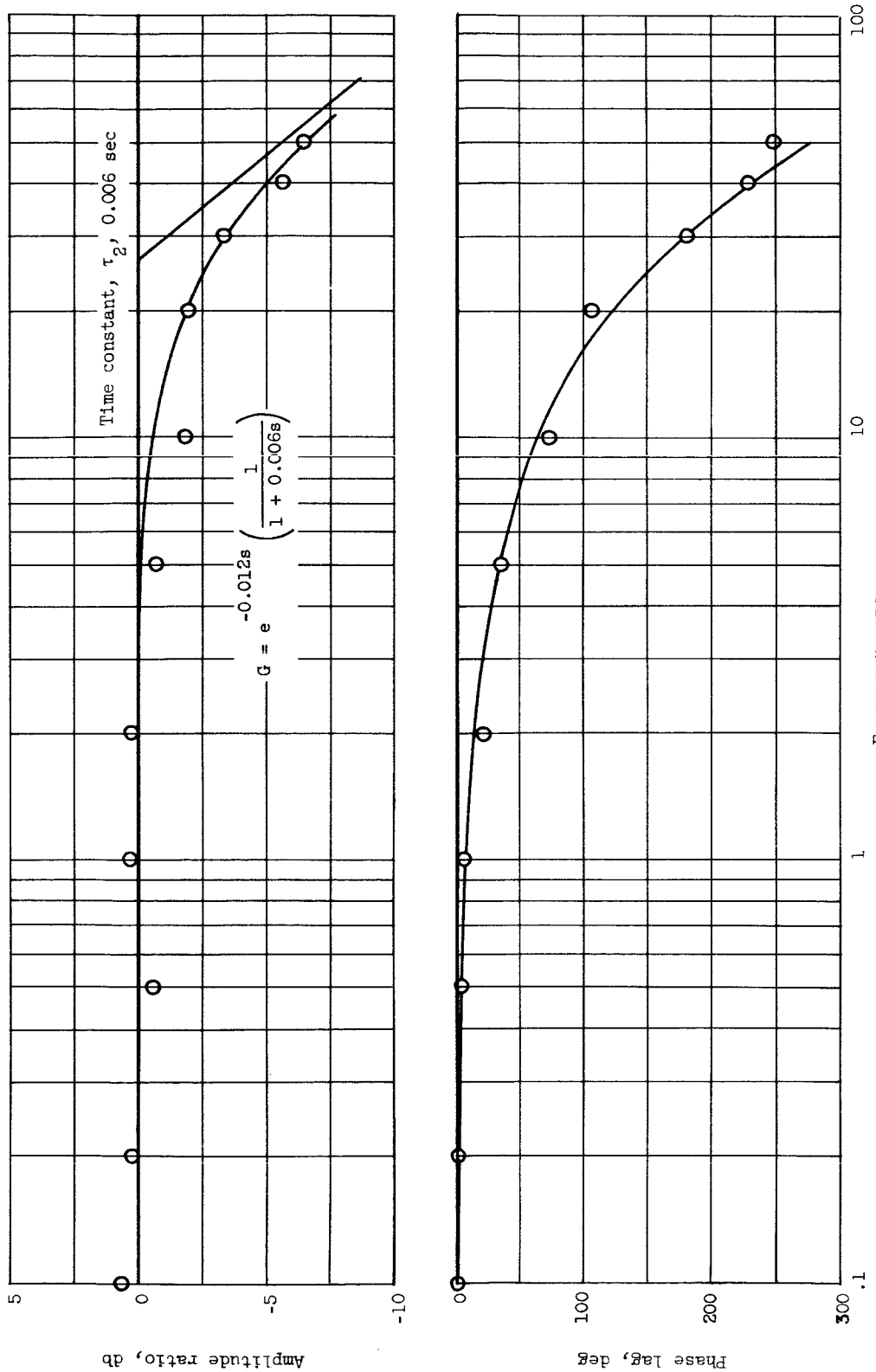

(a) Station 24.

Figure 12. - Frequency response to sinusoidal fuel input for an angle of attack of $+7^{\circ}$. Altitude, 60,000 feet; Mach number, 2.50; base diffuser-exit total-pressure ratio, 9.83; fuel-air ratio amplitude, 0.018.

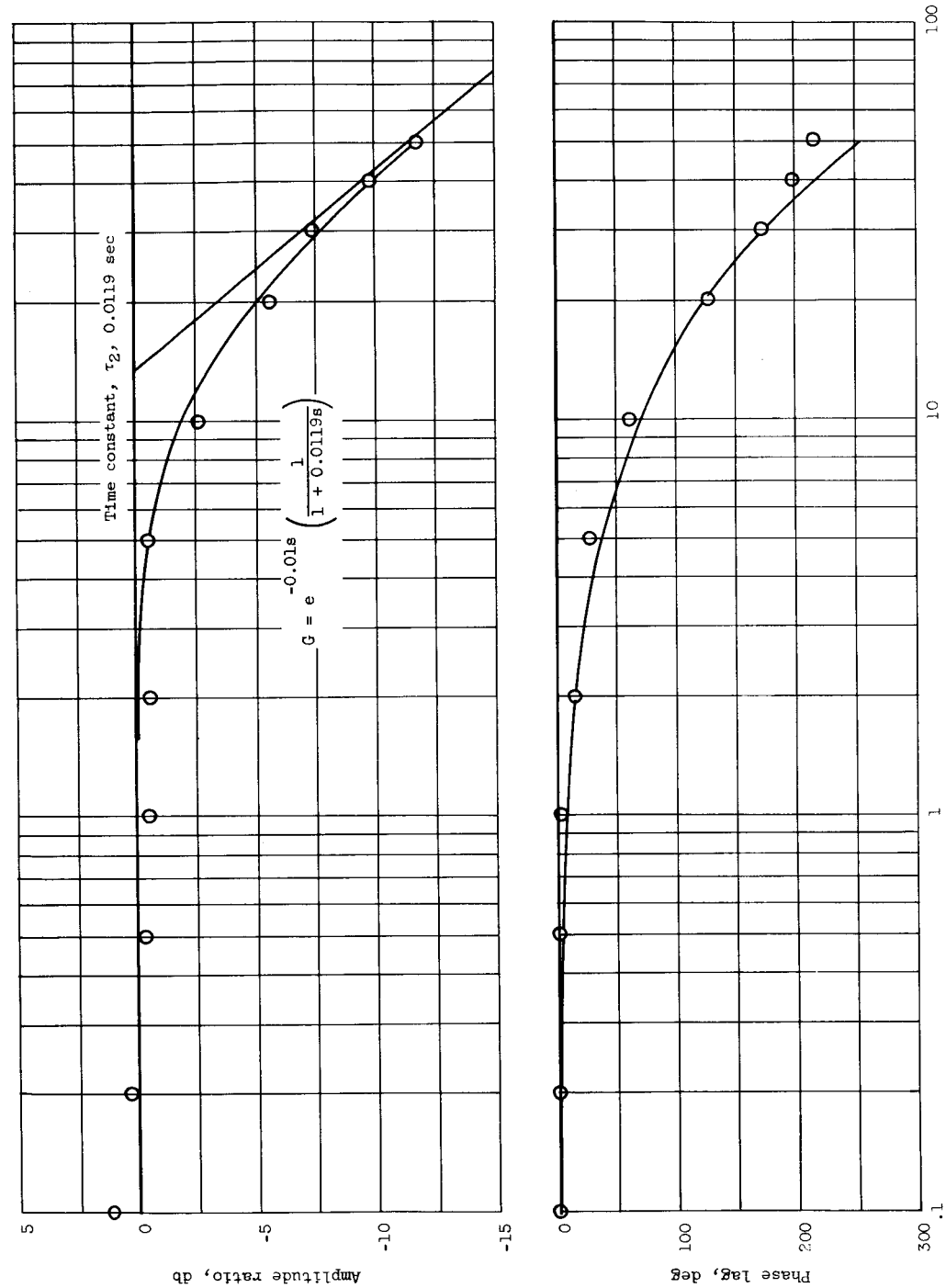

(b) Station 48.

Figure 12. - Continued. Frequency response to sinusoidal fuel input for an angle of attack of $+7^{\circ}$. Altitude, 60,000 feet; Mach number, 2.50; base diffuser-exit total-pressure ratio, 9.83; fuel-air ratio amplitude, 0.018.

4058

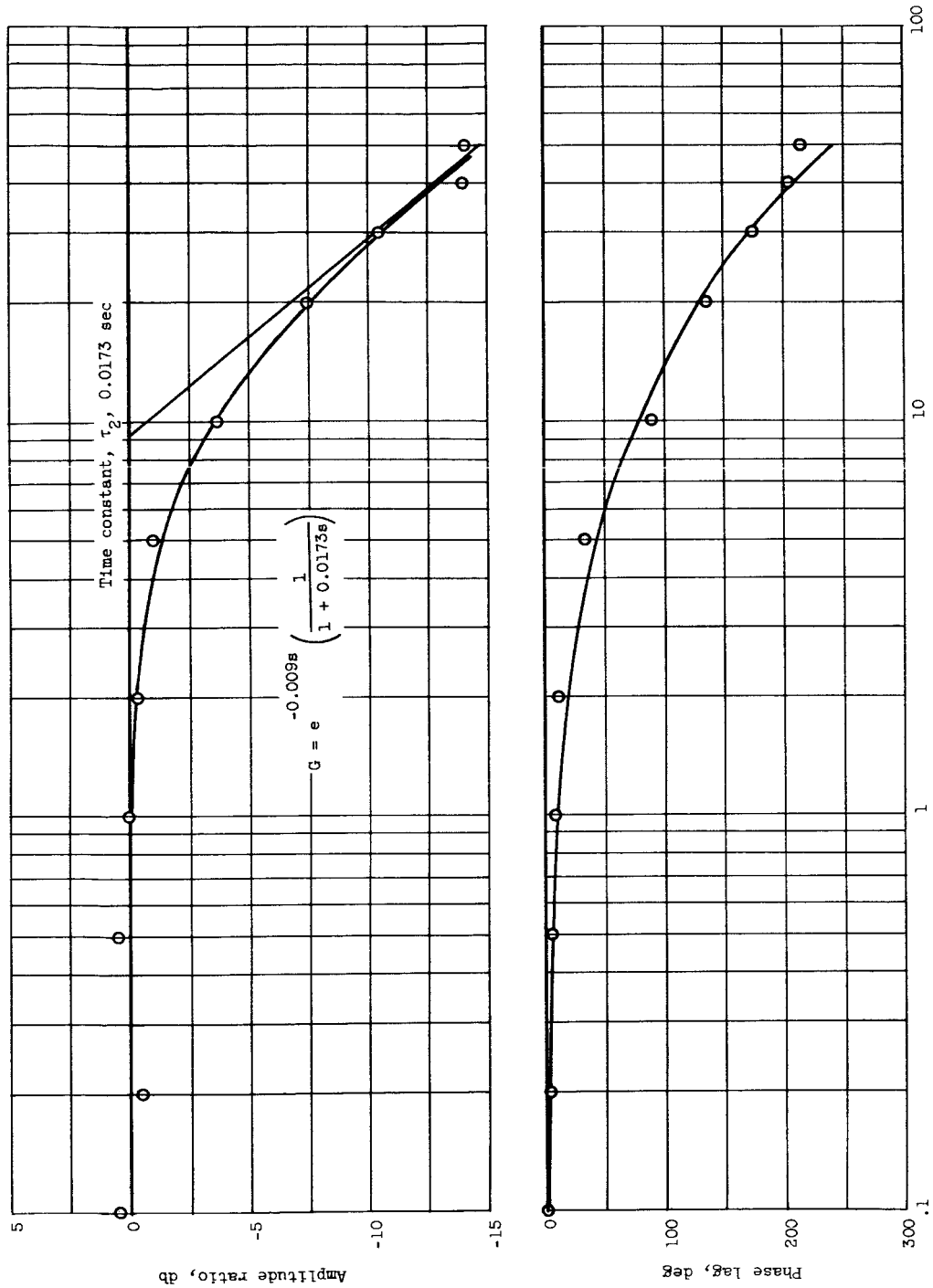

(c) Station 68.

Figure 12. - Concluded. Frequency response to sinusoidal fuel input for an angle of attack of +7°. Altitude, 60,000 feet; Mach number, 2.50; base diffuser-exit total-pressure ratio, 9.83; fuel-air ratio amplitude, 0.018.

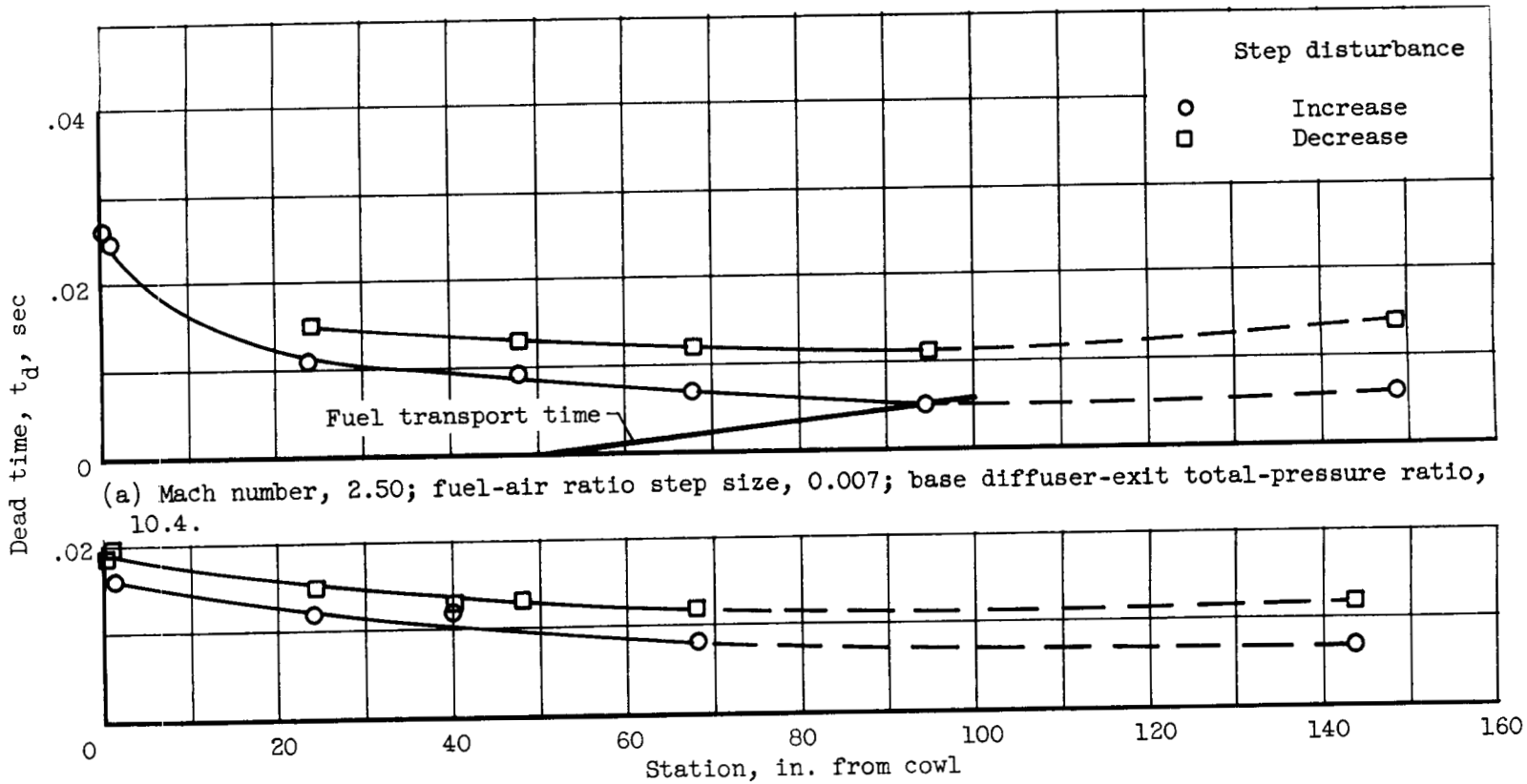

(a) Mach number, 2.50; fuel-air ratio step size, 0.007; base diffuser-exit total-pressure ratio, 10.4.

(b) Mach number, 2.35; fuel-air ratio step size, 0.011; base diffuser-exit total-pressure ratio, 9.15.

Figure 13. - Dead time at various engine stations for step disturbances in fuel flow. Altitude, 60,000 feet; zero angle of attack.

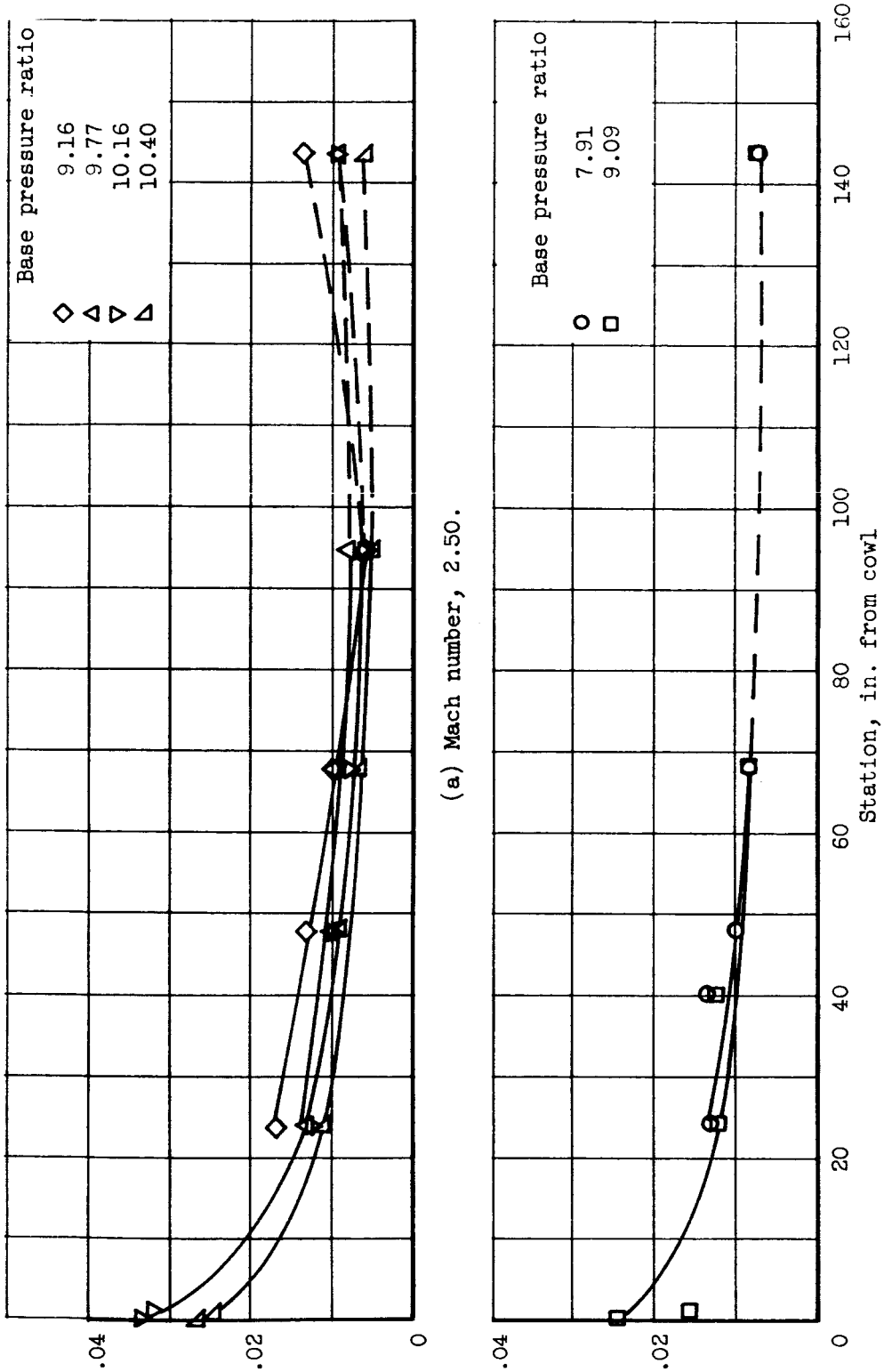

Figure 14. - Effect of base diffuser pressure recovery on dead time for step increase in fuel flow. Altitude, 60,000 feet; fuel-air ratio step size, 0.006; zero angle of attack.

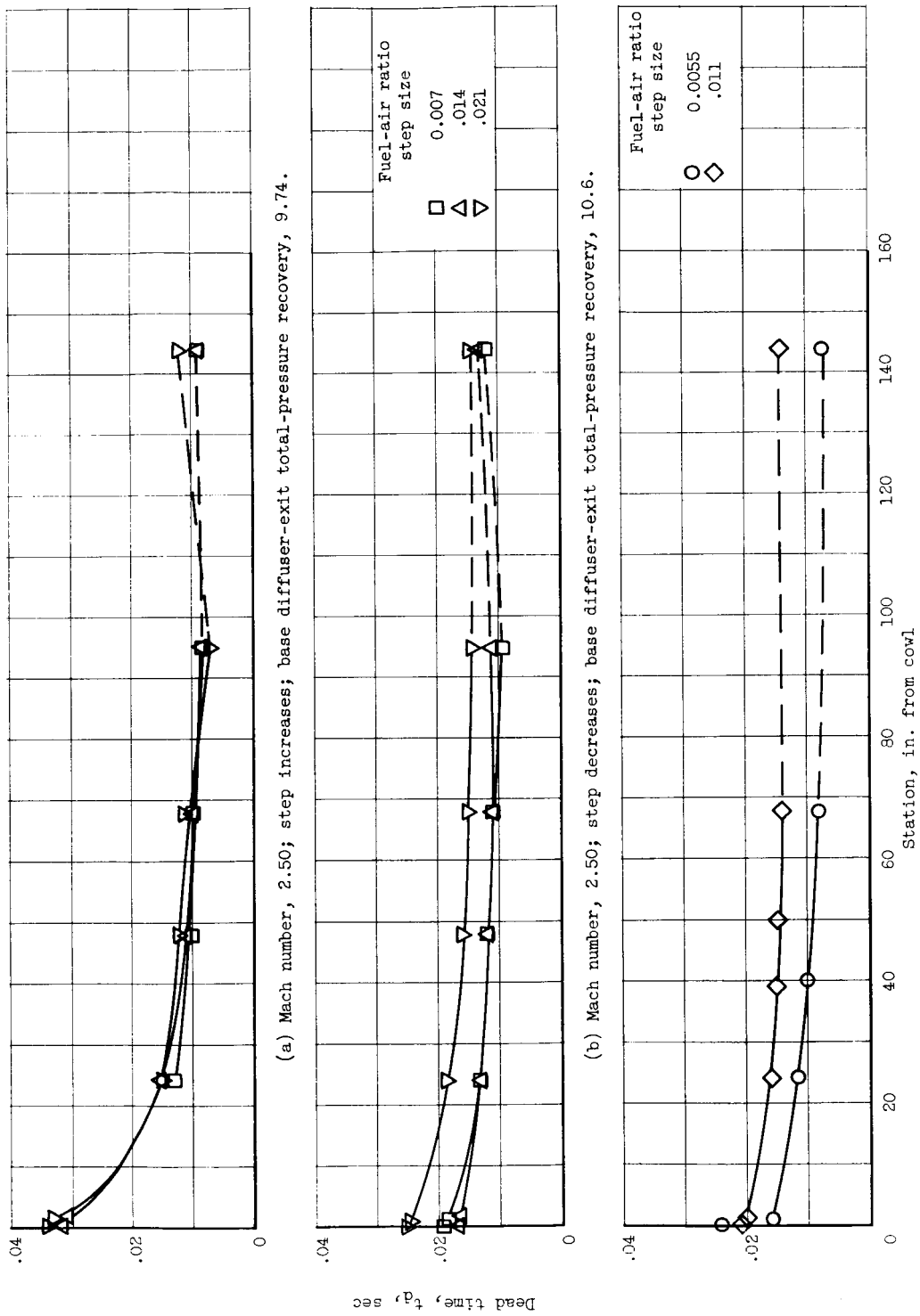

(a) Mach number, 2.50; step increases; base diffuser-exit total-pressure recovery, 9.74.

(b) Mach number, 2.50; step decreases; base diffuser-exit total-pressure recovery, 10.6.

(c) Mach number, 2.35; step increases; base diffuser-exit total-pressure ratio, 9.15.

Figure 15. - Effect of step size on dead time. Altitude, 60,000 feet; zero angle of attack.

NACA - Langley Field, Va.